PROGRAMME:

Eurpean Master in Quality in Analytical Laboratories (EMQAL) 2008-2010

RESEARCH WORK:

Manufacture, characterisation and analytical application of nanomaterials in sensor devices.

Department: Analytical Chemistry.

Student: Chukwuemeka Ajaero **Supervisor: José María Palacios Santander**

Signature: **Signature:**

TABLE OF CONTENTS

LIST OF TABLES.

LIST OF FIGURES

ACKNOWLEDGEMENTS

I would like to express my sincere gratitude to my research supervisor José María Palacios Santander, for his continuous support, motivation and outstanding scientific guidance and patience throughout this research work, supporting me in this work and giving me his opinion and directives every time I needed such. I would also like to thank Laura Cubillana Aguilera and Prof. Ignacio Naranjo Rodríguez for their kind assistance. Finally, I also thank Prof. José Luis Hidalgo Hidalgo de Cisneros as well, responsible of the research group in which I have carried out my research work.

Special thanks also go to the European Commission Education and Culture DG for supporting my graduate research and studies through the Erasmus Mundus studentship. I also want to thank the European Master in Quality in Analytical Laboratories Project Management Team (PMT) for the opportunity to participate in this Erasmus Mundus programme, the EMQAL Co-ordinator Prof. Isabel Cavaco and the Co-ordinator of EMQAL in University of Cadiz Prof. Miguel Palma Lovillo and those who taught me in the Erasmus Mundus programme for the knowledge and skills gained through this programme.

I also want to thank my colleagues in the EMQAL 2008 programme, Charles Kosore, Samson Kilaza, Anteneh for being there giving me support. Mention also should be made of Leo, Belachew, Fasil, Teeka, Kumar, Moosa, Jelena, Rufy, Liping, Yingxu, Leire, Joana, Marta, Anu, Rami, Christy, Sintayehu, Saif, Glauce and Phoebe for those enjoyable moments and for being such good friends and coursemates. Worthy of thanks are my friends Joaquín Crespo Rosa, María Franco, Roberto, Laura, Miguel, Sandra who at one time or the other were my Spanish language teachers helping me to learn the language where I left off in the intensive language course and all who have shared some hours in the lab with me. I would also like to thank the other staffs and people in the Department of Analytical Chemistry, more than once have given me their help and support.

I also want to thank my friends Ugochukwu and his Family in Denmark, Mrs.Rita Oze, Chike Nweze, Amara Egwim, Ndui Aikayo, Henrik, Olawumi Makinde, Ana Paula, Ana Laura, Roger, Ley, little Kamil, Yahil (yahaya), Sergio and others numerous to mention.

I want to thank my wonderful parents, Chief (Sir) and Lady E. U. Ajaero, for giving my education and life a facelift, and my siblings Vera, Anita, Uche, Chidumem and Ikenna for being behind me all this time. I can not forget my uncles and their families namely Dr. B. N. Ajaero KSM and Chief (Sir). F. C. Nwokoro KSJ, thanks for your contribution in helping me to attain this level.

I also want to thank those people I have known, for giving me all their support, share their opinions, help in the work we have done since the beginning of my programme right from University of Algarve, Faro, Portugal and the entire staff of the Department of Chemistry at the Federal University of Technology, Owerri, Nigeria, Prof.E.N.Ejike, and Dr.E.E.Oguzie for being there and sharing my life both personally and professionally. Worthy of thanks also is Mrs.Ann Udunwa.

Finally, I thank God for his divine mercy throughout my study period; my sincere gratitude goes to my wonderful friend Wahz for his guidance.

ABSTRACT

The main objective of this study consisted of developing a new type of amperometric sensors based on depositing gold nanoparticles obtained from two different synthetic routes (thermal and ultrasonic methods) on the surface of a Sonogel-Carbon matrix, in order to build electrochemical devices.

UV-visible spectroscopy was employed to study the time stability of the gold nanoparticles, with the aim of comparing between the two syntheses. As expected from theoretical considerations both types of gold nanoparticles showed one peak at 525 nm corresponding to the surface plasmon resonance effect typical of this kind of nanomaterials.

Cyclic voltammetry (CV) and differential pulse voltammetry (DPV) were used to investigate electrochemical behaviour of AuNPs-modified Sonogel-Carbon electrodes at different configurations with the aim of comparing their performance. The AuNPs-modified Sonogel-Carbon electrodes showed significantly enhanced peaks with respect to the unmodified Sonogel-Carbon electrodes. Furthermore, the peak currents increased linearly with the square root of the scan rate indicating that electrochemical reactions were controlled by diffusion process.

Differential pulse voltammetry under optimized conditions showed good reproducibility and repeatability towards ascorbic acid. The detection and quantification limits were also determined.

The AuNPs-modified Sonogel-Carbon electrodes and unmodified Sonogel-Carbon electrodes were structurally characterized with Optical Microscopy (OM), Scanning Electron Microscopy (SEM) and X-ray Energy Dispersive Spectroscopy (EDS). Information about the size distribution and shape of the gold nanoparticles was obtained thanks to Transmission Electron Microscopy (TEM) technique.

The new amperometric sensors developed throughout this research work were also used for the determination of ascorbic acid in apple juice for babies, giving regular results.

1. State-of-the art

1.1. Objectives

The main objective of this research work consists of learning to manufacture carbon-based electrochemical sensor devices, modified with metal nanoparticles in order to characterize the sensor devices structurally (on its surface) and electrochemically, using different techniques for each purpose. The research study includes the first attempts for the application of the amperometric sensors developed throughout this research work to real samples.

The goals to be achieved with this line of research are:

- First of all, to compare two different syntheses of gold nanoparticles in terms of simplicity and fastness of synthesis, time stability and size of the nanoparticles.
- Secondly, to evaluate the possibility of modifying Sonogel-Carbon electrodes with these gold nanoparticles.
- In third place, to characterize these new gold nanoparticles-modified amperometric sensors both electrochemically and structurally.
- And finally, to test the performance of these electrodes at different configurations when determining certain analyte, namely ascorbic acid. Some tests have been done to determine this analyte in apple juices for babies.

1.2. Nanomaterials

Nanomaterials are materials structured on the sub-hundred nanometer scale, which may be assembled and organised to yield nanodevices and nanosystems that possess new or improved properties.

Because of their small size, nanomaterials have unique properties. Their physical, chemical, and mechanical properties are different from the properties of ordinary size materials. For example, they may have difference in structures, surface

compositions, shapes, and optical and electrical properties. Nanomaterials are exceptionally strong, hard, malleable at high temperatures, and chemically active. All physical and chemical properties are size dependent, and the properties of materials on the nanosize scale have important consequences in wide ranging fields. Exploiting nanoscale behavior will eventually lead to development of devices that can selectively attack diseased cells, increase computer speed or improve chemical and biological sensors. The composition, size, shape and environment of nanosized particles strongly influence their ultimate utility. [1,2].

1.3. Sol-gel composite electrodes

Nowadays, the manufacture and application of graphite based sol-gel electrodes have attracted significant interest and importance in the bid to establish alternatives to other solid electrodes [3-7]. Meritorious features include high conductivity, relative chemical inertness, good mechanical properties, physical rigidity, renewable surface, amenable chemical or biological modification, and stability in various solvents [8,9]. They have particularly favourable electrochemical properties, as a wide operating range of voltage window and very low load capacity observed (C_{obs}), compared with other carbon electrodes. In addition, the electrodes respond directly to a broad group of organic compounds and various metal ions which, along with the properties mentioned, makes them very suitable for use as electrochemical sensors.

In addition, the procedure developed for the fabrication of the electrodes is easy; by simply adding graphite to the precursors solution, conductivity is conferred to it and the mixture is readily malleable, so that any configuration can be virtually obtained. Furthermore, there is also the opportunity to tailor the structures by controlling the chemistry of the sol-gel process, thus yielding materials with very different properties [10]. The sol-gel process is a chemical synthesis technique. Several research works have accounted for the application of sol-gel technique [11-18].

1.4. General procedure for manufacturing Sonogel.

The sol-gel process is a wet-chemical technique starting from a chemical solution which acts as the precursor for an integrated network (or *gel*) of either discrete particles or network polymers. Typical precursors are metal alkoxides and metal chlorides, which undergo various forms of hydrolysis and polycondensation reactions. The formation of a metal oxide involves connecting the metal centers with oxo (M-O-M) or hydroxo (M-OH-M) bridges, therefore generating metal-oxo or metal-hydroxo polymers in solution. Thus, the sol evolves towards the formation of a gel-like diphasic system containing both a liquid phase and solid phase whose morphologies range from discrete particles to continuous polymer networks. Most times, acid or base catalysts are used, which accelerates the onset of hydrolysis, and to achieve homogeneous aqueous and organic phases.

The initial hydrolysis of the alkoxide, followed by condensation reactions in localized regions, results in a suspension of colloidal particles called sol. The polycondensation of the particles increases the inter-connection between them, so that the viscosity increases rapidly and leads to the formation of a rigid network, called wet polymer gel, consisting essentially of siloxane units (SiO_2); in most cases, units are connected by oxygen bridges.

The early stages of hydrolysis and polymerization produces alcohol and water, respectively, which together with the excess of water that we added in the precursor mixture and humidity of the external environment, are housed inside the network that has formed. The reaction products are released as the process moves forward, though not completely free. Even after the point of gelation, in which the entire volume of the solid is interconnected, the gel structure and properties continue to evolve as there is solvent in the pores and the gel remains wet. In addition, polycondensation reactions continue occurring, thereby extending the crossover.

As a result, dynamic way, the gel undergoes a progressive spontaneous contraction, resulting in the expulsion of pore fluid, and there is an increase in the internal forces of the gel, diminishing the pore size. However, most of the water and alcohol

generated during the process are retained on the network during gelation. Therefore, a gel aging can be defined as a vitreous material with an internal aqueous solid-phase.

Once this gel get aging, they are subjected to a mild heat treatment (generally less than 100^{o}C), obtaining a dry gel, called xerogel which undergoes no further fluid loss and can be considered stable over time. If instead of subjecting the gel to this smooth process, it is followed by thermal treatment at high temperatures, there is a densification of the material, leading to a totally compact crystal.

The sol-gel process can be classified in three main stages from chemical point of view:

1. Preparation of the sol: colloidal dispersion of particles in a liquid.

2. Gelification of the sol: this step results in a rigid network of inter-connected microscopic pores and polymer chains.

3. Removal of solvent in the network: at this stage, a solid condensate is obtained.

All the above process takes place at room temperature, which is one of the main characteristics of this type of synthetic route.

As a result, different species can be introduced during the first stage, even in the case of labile species. Certain solids synthesized via sol-gel have capacity for ionic and electronic conduction and this property makes them suitable for being used in conventional electrochemical techniques such as voltammetry.

The filling of capillaries is performed by inserting them within the heart of the sol in the container, rotating in both directions with respect to the vertical axis, and trying to avoid the gaps that may remain, what is relatively complicated, taking into account the high viscosity of the sol and the small diameter of the capillary; however, proper distribution of the sol-gel along the glass tube is ensured.

Once filled, a copper wire is introduced in each capillary tube in order to compact the material inside. The pressure is maintained with the thread until a small amount of sol falls outside the capillary, thus facilitating subsequent grinding and polishing.

In the moments before the measure the material that protrudes from the base of the electrode are removed using fine grit sandpaper. If the excess is large, first coarse sandpaper can be used to accelerate the process and subsequently the fine grain one. Then the resulting surface is rubbed with a glossy paper placed on a smooth surface. Thus, the surface is polished (shiny and smooth). With regard to electrical contact (Cu wire), it is set once the material is hardened, ensuring its perfect immobilization.

1.5. Factors affecting the sol-gel process.

The microstructure of a material obtained by sol-gel process depends on the interaction of a large number of process parameters, and variation of more than one simultaneously can lead to results quite complex. In general, the most important factors are those that influence the rates of hydrolysis and condensation, since during these stages, which originates the sol, are established, somehow, the final factors that will influence the gel. These factors have been studied in earlier works and are listed below.

The factors that rely primarily on the kinetics of hydrolysis and condensation reactions are:

- Type of alkoxide precursor.

- Initial molar ratio alkoxide precursor:water.

- Type (acid or basic) and concentration of the catalyst.

- Type of solvent.

- Temperature.

1.6. Ultrasound synthesis of sonogel.

Depending on the effect that is being studied, applications of ultrasound can be classified in two types.

The first area is related to the effect of environment on the wave [19,20], while the second area focuses on studying the effect of the wave on the environment, such as

emulsion formation, based on the use of high power ultrasounds and/or low frequencies. Studies conducted on this last area [21,22] agree that it must take place the phenomenon of ultrasonic cavitation for wave effects on the environment to become apparent.

A general form of ultrasonic cavitation and the formation of a new surface within the liquid by the irradiation of ultrasound waves can be defined.

Applying ultrasound in immiscible systems can expand the interface between both phases significantly, facilitating the exchange of molecules between them, thus obtaining extremely fine emulsions. The application of ultrasonic to precursor alkoxide-water mixture that is immiscible in the presence of an acid catalyst is an alternative to synthesize different gels, without solvents, called sonocatalysis. By using this method materials are obtained with different characteristics, called sonogels [23].

The ultrasonic waves will act on the liquid-liquid interface of the alkoxide-water mixture which results in the formation of bubbles dissolved in the liquid, reaching extremes of pressures and temperatures (in the bubbles). During the collapse of these bubbles produced by hydrolysis, a homogeneous liquid is yielded which subsequently polymerize to form the gel.

The cavitation induced by the use of ultrasounds, together with the absence of solvent, constitutes an exceptional set for achieving the sol-gel process, resulting in the existence of specificity in sonogels such as: high density fine texture, and homogeneous structure, among others.

For the preparation of a sonogel, hydrolysis of the precursor mixture is done; then it is subjected to ultrasonic waves in an open glass container. For this purpose, the simplest and most accessible equipment would be an ultrasonic bath. However, it has the disadvantage that the power delivered by the device varies depending on the size of the bath, the reaction vessel and its position within the bath, so that energy is dispersed over a larger volume, so ultrasounds levels required for cavitation are not enough in the reaction mixture.

Without doubt, the most effective method for transmitting ultrasound energy to the mix is the direct immersion of a probe into the liquid reactant. The function of this probe is to amplify the vibrational movement originated in the generator (which is often insufficient for practical cases). The material for the manufacture of acoustic sensors is a titanium alloy. Thanks to this the direct immersion of the probe into the reaction system can generates ultrasonic power much higher than that reached in the bathroom, because in this system there are no energy losses in the transfer of ultrasounds between the probe and the reaction mixture. The amount of energy supplied to the system is determined by the time of insonation which is an additional parameter to control the properties of sol-gel.

Compared with traditional methods of obtaining gels, which may include the presence of an alcohol as solvent, the first noticeable effect is the considerable decrease in the gelification time. This parameter decreases further when increasing the dose of ultrasounds applied to the mixture. When using the classical method, the dilution existing at the beginning causes a large decrease in the density of the gel due to excessive porosity resulting from the removal of the solvent. This effect is not desirable when you require high-density matrices suffering from low volume contraction.

1.7. Application of ultrasound in the synthesis of gold nanoparticles.

The major aspect of nanotechnology is the development of synthesis of metal nanoparticles. In this sense, nanosized particles of noble metals, especially gold nanoparticles (AuNPs), have received great attention as a result of their attractive electronic, optical, and thermal properties, as well as catalytic properties and potential applications in the fields of physics, chemistry, biology, medicine, and material science and their different interdisciplinary fields [24]. Therefore, the synthesis and characterization of AuNPs have attracted significant attention from a fundamental and practical point of view. The particles should be stable chemically without undergoing degradation such as partial oxidation or undesired sintering.

The synthesis of gold nanoparticles with diameters ranging from a few to several hundreds of nanometres is well established in aqueous solution as well as in organic solvents. In typical synthesis, gold salts such as $AuCl_3$ are reduced by the addition of a reducing agent which leads to the nucleation of Au ions to nanoparticles. In addition, a stabilizing agent is also required which is either adsorbed or chemically bound to the surface of the Au nanoparticles. This stabilizing agent (often also called a surfactant) is typically charged, so that the equally charged nanoparticles repel each other so that they are colloidally stable. Au nanoparticles protected via self-assembly (in two or three dimensional lattices) are also promising for the construction of nanodevices and nanocircuits [25,26].

For the most common synthesis route in aqueous solution, citric acid serves first to reduce the gold salt and thus to trigger nucleation; and secondly, due to its adsorption on the particles surface, it provides colloidal stability to the particles by its negative charges [27].

Extensive studies [28-32] of aqueous sonochemistry have shown that the chemical effects of ultrasounds are attributed to cavitation. The collapse of the cavities which occurs during ultrasonic irradiation leads to the decomposition of water molecules to hydrogen atoms and hydroxyl radicals owing to the production of high temperatures and pressures.

Over the past decade, straightforward, economically viable, and 'green' synthesis of nanoparticles has been paid wide attention in the emerging areas of nanoscience and technology to yield mono-dispersed metal and semiconductor nanoparticles at ambient temperature and within a short time [33]. These synthetic routes have lead to the application of ultrasounds (sonocatalysis) in the synthesis of nanoparticles. One of the gold nanoparticles used in this research work was synthesized following this approach. The application of green synthetic approach in synthesis of gold nanoparticles has been reported in several works [34-39].

Other synthetic approach for gold nanoparticles employed in this work was the thermal method.

1.8. Comparison between ultrasonic and thermal methods of synthesis of gold nanoparticles.

Ultrasounds synthesis route has some major advantages when compared with the thermal method of synthesis of our nanoparticles.

The ultrasonic method is associated with local high temperatures and pressures created during the bubble collapse with the rapid cooling rate (> 10^9 K·s^{-1}), greater than those obtained by conventional quenching technique (10^5 to 10^6 K·s^{-1}), which enables the formation of colloids as well as the formation of nanoparticles [40,41]. The high temperatures, pressures and cooling rate attained during acoustic cavitation lead to many unique properties in the irradiated solution [42].

Secondly, kinetics and regiospecificity of ultrasonic degradation are different from those of thermal processes (classical/conventional method). Thermal degradation produces cleavage at random points along the chain of inorganic polymers (*e.g.* poly(polyorganosiloxanes) and polyorganosilanes) and various polymers in aqueous media, whereas ultrasonic degradation is much more specific, with cleavage occurring preferentially near the middle of the chain of polymers [43,44].

1.9. Background and current status

The sol-gel technology finds numerous applications in the field of chemistry: optically transparent matrices [45,46], electrochromic devices [47,48], construction of cathodes [49,50], supports for solid phase extraction (SPE) [51,52] and liquid and gas chromatography [53,54]. Applications of this technology in the area of electroanalysis are relatively recent and require a special type of sol-gel materials which has to be conductors of electric current [49]. The substances most commonly

used to provide electrical conductivity in sol-gel materials are finely divided metals such as gold dust, and graphite.

A sol-gel electrochemical material can be defined as a mixture in which the inorganic matrix is modified with conductive material, in order to be used as an electrode in an electrochemical system. We could also consider the existence of a category within the field of chemically modified electrodes (CMEs), which include electrodes modified with oxides synthesized by sol-gel processes, specifically with silicon oxide (SiO_2-Monolithic).

Research related to SiO_2-Monolithic began slowly in the early 90s, despite the appropriate characteristics of these materials for accumulating electroactive species prior to electrochemical detection, for instance, absorption capacity, chemical acid/ base and thermal stability. An example is the application of electroactive materials obtained via sol-gel in the form of thin films, which were developed by Lundgren and Murray [53] in 1987. These investigations showed a rapid rise in 1994 in the field of amperometric biosensors thanks to the discovery of the possibility to incorporate enzymes in the inorganic matrix keeping intact their biological activity. More recent applications in electroactive materials related to the work carried out by Maruszewski can be found in [55] and Kim [56].

By doping the sol-gel silica at the beginning of or during the polymerization process, Hsueh and Collinson [57] produced electrodes with a glassy carbon organically modified silica coating with-NH_2 or-COOH and voltammetrically characterized by finding a remarkable capacity for ion exchange materials, attributed to electrostatic interactions between the analyte and the acidic or basic function of the organosilane. The biggest advantage that organically modified sol-gel material has consists of the combination of the properties of inorganic crystals with the intrinsic properties of organic molecules. Wang et al. [58] extended this possibility by making composite electrodes and carbon sol-gel modified with dimethylglyoxime and using voltammetry to detect traces of nickel, thus exploiting the same device on the advantages of sol-gel chemistry and electrochemical pre-concentration. Later he

used many organic modifiers; two of the most recently employed have been polydimethylsiloxane (PDMS) [59] and tetrapropiortotitanate (TPOT) [60].

Y. Guo and Ana R. Guadalupe [61] developed in 1998 a process for preparing graphite composite electrode/sol-gel precursor mixture applied with silk screen-printing techniques. No alcoholic co-solvents and catalysts were used, but only a wetting substance that performs these functions. The manufacture of the modified electrodes proceeds in one step by this technique. The reproducibility of results obtained in the applications of these electrodes as sensors and biosensors is not very good, maybe because of the homemade print device.

In the literature, examples of specific use of electrochemical sensors and biosensors in the field of applied analysis, such as analysis of food, beverages and drinking water control, showing special interest in species that establish properties of foods and beverages that are directly related to its flavour and stability can be found in [62,63]. The wide variety of analytes and the great diversity of materials is an added problem to this type of application, apart from those related to the sensor itself, as its stability over time and sensitivity of their response.

With regard to the structural characterization of sol-gel materials, numerous research groups have gone into this topic. Outstanding among all the groups is the research led by Esquivias (University of Cadiz) [64] and Vollet (University of Brasilia) [65].

A wide range of techniques used in structural characterization exists, which can be used independently to obtain data from a physical characteristic or particular structural material or jointly, with the aim of achieving a more complete characterization. In this case, we can highlight spectroscopy, different types of electron microscopy [66] and the techniques of X-ray diffraction [67], among others.

The collaboration of various research groups at the University of Cadiz, Spain has resulted in the recent development of a new material and electrodes/sensors, which has been a major development internationally. This has resulted in the publication of several articles in reputable international journals.

The usual procedures to synthesize sol-gel materials for electrodes involve acid catalysis, requiring the precursor mixture in the presence of an alcoholic solvent, times of insonation greater than 10 minutes (at least) in an ultrasonic bath for starting the hydrolysis. The subsequent evaporation of the solvent causes a marked reduction in the volume of material with pore formation, which is completely undesirable for the preparation of solid electrodes.

The most recent proposal done at University of Cadiz is quite different from the manufacturing method, and is based on the use of high-energy ultrasounds applied directly on precursors. In this way, ultrasonic cavitation occurs, which promotes acid hydrolysis in the absence of any additional solvent, yielding a unique phase only in a few seconds. This is known as sonocatalysis. The mixture with spectroscopic grade graphite has led to a new type of sol-gel material: the Sonogel-Carbon material.

1.10. Voltammetric techniques.

The experimental part of this work involves the use of two voltammetric techniques. Thus, this section has been included in order to describe the general foundations of the voltammetry and the characteristics of both techniques.

Voltammetry covers a series of electroanalytical methods developed from polarography. In fact, voltammetry arose as a response to the multiple challenges posed by the use of polarographic techniques in sensitivity and selectivity.

The main characteristic of dc polarography is based on the use of a mercury drop electrode as working electrode, so if the working electrode is not this, then the technique is called voltammetry.

The common characteristic of all voltammetric techniques is that they involve the application of a potential (E) to an electrode and the monitoring of the resulting current (i) flowing through the electrochemical cell. In many cases the applied

potential is varied or the current is monitored over a period of time (*t*). Thus, all voltammetric techniques can be described as some function of *E*, *i*, and *t*. They are considered active techniques (as opposed to passive techniques such as potentiometry) because the applied potential forces a change in the concentration of an electroactive species at the electrode surface by electrochemically reducing or oxidizing it.

The various voltammetric techniques show many analytical advantages: excellent sensitivity with a very large useful linear concentration range for both inorganic and organic species (10^{-12} to 10^{-1} *M*), a large number of useful solvents and electrolytes, a wide range of temperatures, rapid analysis times (seconds), simultaneous determination of several analytes, the ability to determine kinetic and mechanistic parameters, a well-developed theory, and thus, the ability to reasonably estimate the values of unknown parameters, and the ease with which different potential waveforms can be generated and small currents measured.

Analytical chemists routinely use voltammetric techniques for the quantitative determination of a variety of dissolved inorganic and organic substances. Inorganic, physical, and biological chemists widely use voltammetric techniques for a variety of purposes, including fundamental studies of oxidation and reduction processes in various media, adsorption processes on surfaces, electron transfer and reaction mechanisms, kinetics of electron transfer processes, and transport, speciation, and thermodynamic properties of solvated species.

The electrochemical cell, where the voltammetric experiment is carried out, consists of a working (indicator) electrode, a reference electrode, and usually a counter (auxiliary) electrode. In general, an electrode provides the interface across which a charge can be transferred or its effects felt. Since the reaction or transfer of interest takes place at the working electrode, whenever we refer to the electrode, we always mean the working electrode. The reduction or oxidation of a substance at the surface of a working electrode, at the appropriate applied potential, results in the mass transport of new material to the electrode surface and the generation of a

current. Even though the various types of voltammetric techniques may appear to be very different at first glance, their fundamental principles and applications derive from the same electrochemical theory [68].

1.10.1. Cyclic voltammetry.

The cyclic voltammetry can be considered an extension of the linear sweep voltammetry. It is based on making the working potential, (the values oscillating between two limits from a minimum to a maximum in a given time) to grow linearly, and then to descend again to the minimum value in the same minimum-maximum period. The sequence constitutes a cycle figure 1.1. The part of the cycle in which the potential is increasing in positive direction is called positive sweep; the half cycle with decreasing the potential sweep is called negative.

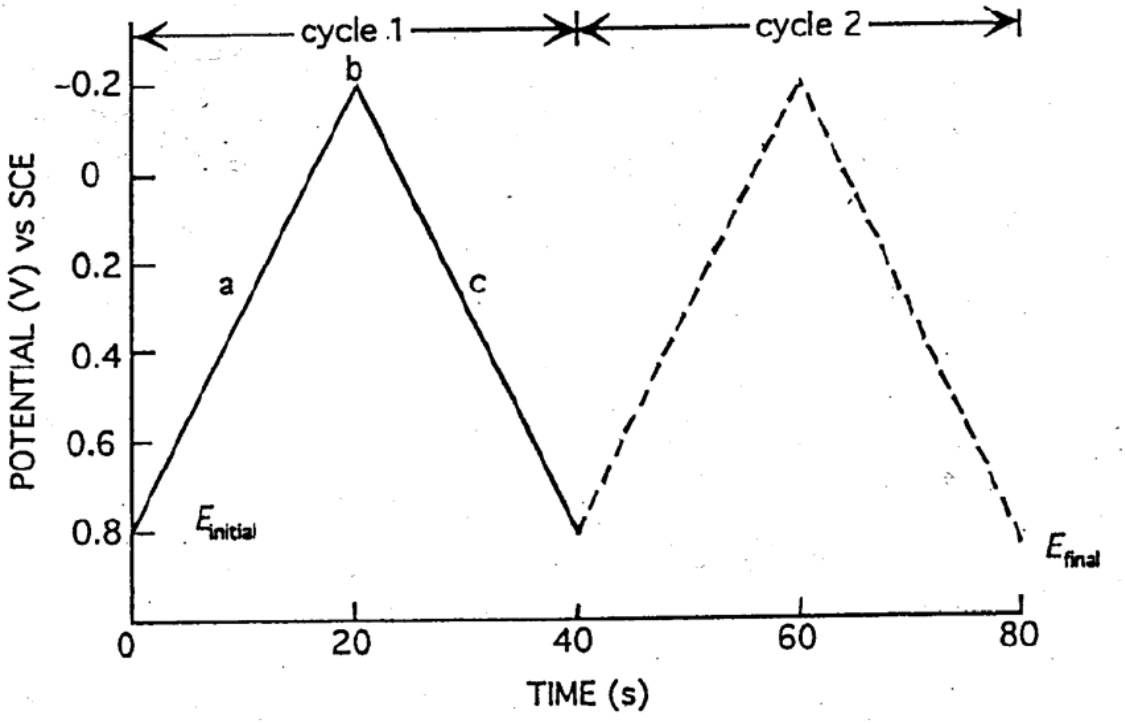

Figure 1.1: Typical excitation signal for cyclic voltammetry.

The scan profile is usually defined in terms of the redox couple of interest in the experiment. The current intensity measures are carried out throughout the cycle and its representation against the applied potential results in a graph called voltammogram (figure 1.1.). The measures of intensity for the anodic and cathodic peaks are usually carried out by extrapolating the base line of each half cycle just before each peak starts to emerge, so that this is the main drawback of cyclic voltammetry, since the values of intensity obtained are not always reliable.

With regard to the application, it is often the first technique used when an electrochemical study is intended. The main reason is that this is probably the most versatile electrochemical technique to study mechanisms for effective redox systems. It makes sweeps of potential and identifies the presence of a redox couple in the electrolytic medium.

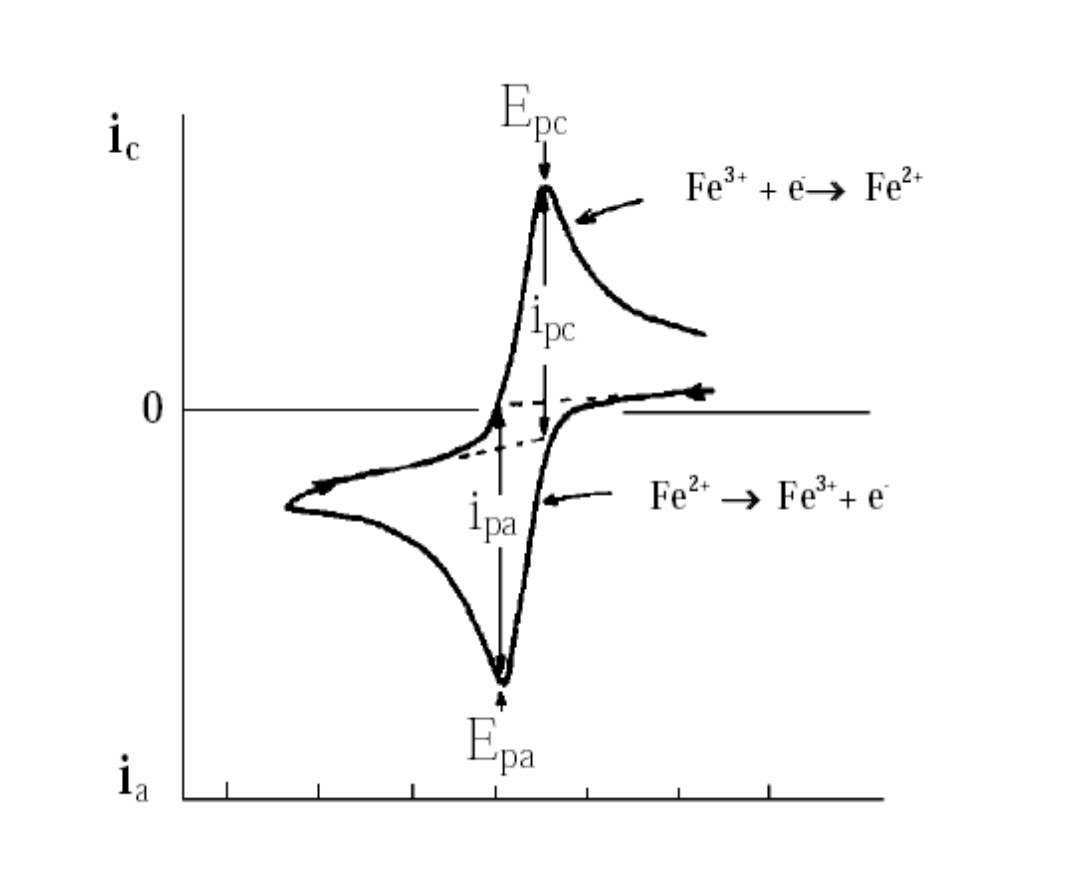

Figure 1.2. Cyclic voltammogram of the redox couple Fe2+/Fe3+ in H2SO4 1M.

Once found, this redox couple can be characterized by the peak potential of the voltammogram, and the analysis of the possible changes caused by varying the sweep speed of potential as well. It is therefore useful when studying reversible electrochemical systems, *i.e.* those in which both redox couple species exchange electrons with the electrode rapidly.

To evaluate the electrochemical behavior of a developed electrode is also common to start using the technique discussed, because, through it, it is possible to know the electrocatalytic field range that can cover the electrode and the current intensity or non-faradaic charging that provides medium electrolyte (in the absence of species). Cyclic voltammetry, along with other voltammetric techniques, is an important tool to carry out, for example, the study of a chemically modified electrode [69].

1.10.2. Differential pulse voltammetry

In general, pulse voltammetric techniques were devised for the purpose of correcting the drawbacks of current polarography. The first one in being developed was differential pulse polarography, and thanks to that, the shortcomings arising from the use of mercury drop electrodes were overcome. Thus, in this technique intensity data are only recorded at the end of the droplife and, by applying pulse potential, the intensity is maximized. Equally, when performing this technique with negligible charge current, most of the values found are dismissed. With such advances it is able to reduce significantly the detection limit and improve the presentation of data.

Moreover, later it was discovered that such improvements were not only applicable to mercury drop electrodes, but also to solid electrodes and mercury film electrodes. Thus, differential pulse voltammetry arose, whose characteristics are described below.

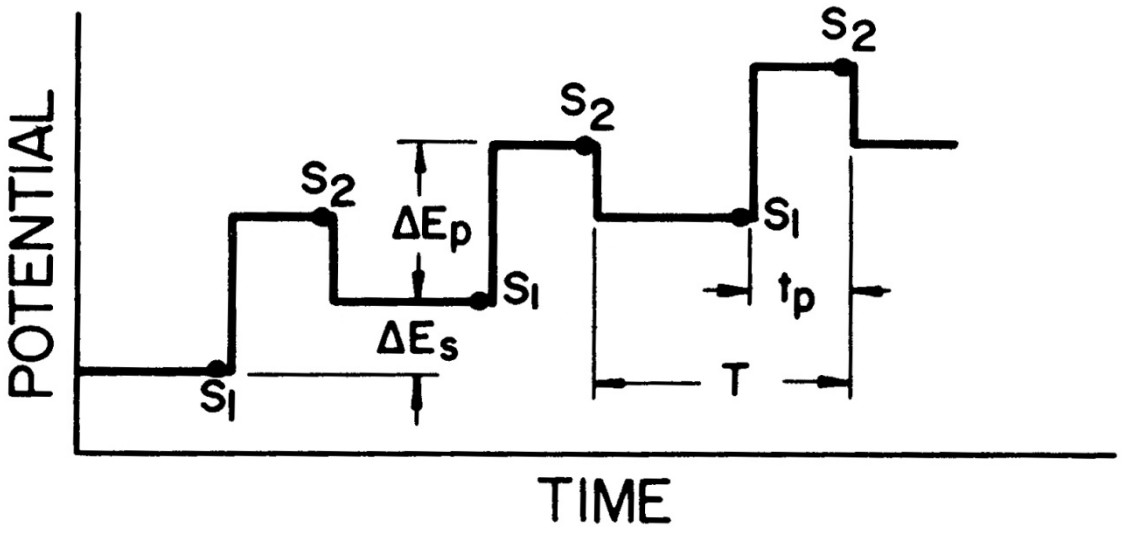

Figure 1.3. Excitation signal in differential pulse voltammetry.

A full description of this technique will be done taken into consideration figure 1.3. The technique involves the application (overlay) of a constant potential pulse (ΔE_p) of duration t (s) at the end of each step ΔE_s height and duration T (s) of a staircase potential. The fact of applying a potential ladder instead of a ramp is due to the advent of digital application to electrochemical experiments, as it is not possible to generate an ideal ramp of potentials, and therefore to perform a series of approximation to produce small steps of potential. However, this approach has the advantage of providing significant improvements through this sampling of current which is done at the end of each step or rung, when Faradaic charging is not missing (and therefore it should only be faradaic current). Values of current are recorded in two points: just before applying the potential pulse (S_1) and at the very end of it (S_2), as shown in the Figure.

When applying a pulsed technique for analytical purposes, the pulse amplitude often increased until 100 mV. Higher values of this parameter provide higher currents, but also cause loss of resolution and increase the load current. Typically it is preferred to utilize values that provide the maximum current value with the lesser

loss of resolution and increase of load current at the same time, 100 mV already achieving a good compromise between these effects [70].

1.11. UV-visible spectroscopy

Ultraviolet and visible spectroscopy (UV-vis) is a reliable and accurate analytical laboratory assessment procedure that allows for the analysis of a substance. Specifically, ultraviolet and visible spectroscopy measures the absorption, transmission and emission of ultraviolet and visible light wavelengths by matter. Ultraviolet and visible spectroscopy (UV-vis spectroscopy) is used to study molecules and inorganic ions in solution.

Ultraviolet and visible light comprise only a small portion of the wide ranging electromagnetic radiation spectrum. Although lower in frequency and therefore lower in energy than cosmic, gamma or X-rays, ultraviolet and visible light are of a higher frequency and, therefore of higher energy, than infrared, microwave and radio waves.

In the practical sense, spectroscopy measures the absorption, emission, or scattering of electromagnetic radiation by atoms or molecules. By such measurements, the type of the atoms or molecules present in a sample, as well as a measure of their concentration or abundance, can be made to an astonishing degree of accuracy.

When ultraviolet or visible light strikes atoms or molecules they can either bounce off or cause electrons to jump between energy levels. Absorption of ultraviolet or visible electromagnetic radiation causes electron to moves from lower energy levels to a higher energy levels. Ultraviolet-visible absorption spectroscopy measures the absorption of ultraviolet or visible light. Since the spectrum of an atom or molecule depends on its electron energy levels, UV-vis absorption spectra are useful for identifying unknown substances.

In UV/visible spectroscopy, a beam of light is split into a sample and reference beams. As its name implies, the sample beam is allowed to pass through the target

sample. Alternately, the reference beam passes through the control solvent or a portion of the solvent that does not contain the actual target. Once the light passes through the target sample of interest it is measured by a special meter termed a spectrometer designed to compare the difference in the transmissions of the sample and reference beams. Double beam UV-visible spectroscopy instruments allow for simultaneous measures of transmissions through the target sample and solvent.

The way by which electromagnetic radiation affects atoms and molecules depends on the energy of the light. The energy is, in turn, dependent upon the frequency of the light. Ultraviolet and visible light promotes electrons into higher energy orbitals.

Special instrumentation is used in UV-vis spectroscopy. Hydrogen or deuterium lights provide the source of light for ultraviolet measurements. Tungsten lamps provide the light for visible measurements. These light sources generate light at specific wavelengths. Deuterium lamps generate light in the UV range (190 to 380nm). Tungsten-halogen lamps generate light in the visible spectrum (380 to about 800 nm). Xenon lamps which can produce light in the UV and visible portions of the spectrum are used to measure both UV and visible spectra.

The wavelengths of ultraviolet or visible light absorbed by a substance result in a unique ultraviolet-visible spectroscopic signature for each substance and can be used as analytical tool.

1.12. Electron microscopy: theory and fundamentals

This section describes the most important aspects of Electron Microscopy (EM), focusing mainly on Scanning Electron Microscopy (SEM), Transmission Electron Microscope (TEM) and the X-ray Energy Dispersive Spectroscopy (EDS), relating to the techniques used in this research. Deeper aspects and more detailed descriptions of the basis for them can be found in [71,72].

Electron microscopes were developed due to the limitations of light microscopes which are limited by the physics of light to 500x or 1000x magnification and a resolution of 0.2 micrometers. In the early 1930's this theoretical limit had been reached and there was a scientific desire to see the fine details of the interior structures of organic cells (nucleus, mitochondria...etc.). This required 10,000x plus magnification which was just not possible using light microscopes.

The transmission electron microscope was the first type of electron microscope to be developed and is patterned exactly on the light transmission microscope except that a focused beam of electrons is used instead of light to 'see through' the specimen. It was developed by Max Knoll and Ernst Ruska in Germany in 1931.

The first Scanning Electron Microscope (SEM) debuted in 1942 with the first commercial instruments around 1965. Its late development was due to the electronics involved in 'scanning' the beam of electrons across the sample. An excellent article was just published in *Scanning* detailing the history of SEMs.

Electron microscopes (EMs) function exactly as their optical counterparts except that they use a focused beam of electrons instead of light to 'image' the specimen and gain information as to its structure and composition.

The basic steps involved in all EMs can be described as follows:

1. A stream of electrons is formed (by the electron source) and accelerated toward the specimen using a positive electrical potential.
2. This stream is confined and focused using metal apertures and magnetic lenses into a thin, focused, monochromatic beam.
3. This beam is focused onto the sample using magnetic lens.
4. Interactions occur inside the irradiated sample, affecting the electron beam.

These interactions and effects are detected and transformed into an image. The above steps are carried out in all EMs regardless of type. A more specific treatment of how the two different types of EMs operate is described in the next subsections.

1.12.1. Scanning Electron Microscopy (SEM)

The scanning electron microscope uses a focused beam of high-energy electrons to generate a variety of signals at the surface of solid specimens. The signals that derive from electron-sample interactions reveal information about the sample including external morphology (texture), chemical composition, and crystalline structure and orientation of materials making up the sample. In most applications, data are collected over a selected area of the surface of the sample, and a 2-dimensional image is generated that displays spatial variations in these properties. Areas ranging from approximately 1 cm to 5 microns in width can be imaged in a scanning mode using conventional SEM techniques (magnification ranging from 20x to approximately 30,000x; spatial resolution from 50 to 100 nm). The SEM is also capable of performing analyses of selected point locations on the sample; this approach is especially useful in qualitative or semi-quantitatively analysis for determining chemical compositions (using EDS).

1.12.2. Scanning Electron Microscopy (SEM)

Accelerated electrons in an SEM carry significant amounts of kinetic energy, and this energy is dissipated as a variety of signals produced by electron-sample interactions when the incident electrons are decelerated in the solid sample. These signals include secondary electrons (that produce SEM images), backscattered electrons (BSE), diffracted backscattered electrons (EBSD that are used to determine crystal structures and orientations of minerals), photons (characteristic X-rays that are used for elemental analysis and continuum X-rays), visible light, and heat. Secondary electrons and backscattered electrons are commonly used for imaging

samples: secondary electrons are most valuable for showing morphology and topography on samples and backscattered electrons are most valuable for illustrating contrasts in composition in multiphase samples (*i.e.* for rapid phase discrimination). X-ray generation is produced by inelastic collisions of the incident electrons with electrons in discrete ortitals (shells) of atoms in the sample. As the excited electrons return to lower energy states, they yield X-rays that are of a fixed wavelength (that is related to the difference in energy levels of electrons in different shells for a given element). Thus, characteristic X-rays are produced for each element in a sample that is 'excited' by the electron beam. SEM analysis is considered to be 'non-destructive'; that is, x-rays generated by electron interactions do not lead to volume loss of the sample, so it is possible to analyze the same materials repeatedly.

The SEM is routinely used to generate high-resolution images of shapes of objects and to show spatial variations in chemical compositions (usually EDS, also BSE).

This instrument is also widely used to identify phases based on qualitative chemical analysis and/or crystalline structure. Precise measurement of very small features and objects down to 50 nm in size is also accomplished using the SEM. Backscattered electron images can be used for rapid discrimination of phases in multiphase samples. SEMs equipped with diffracted backscattered electron detectors can be used to examine microfabric and crystallographic orientation in many materials.

1.12.3. SEM instrumentation

Essential components of all SEMs include the following:

- Electron source ('gun').
- Magnetic lenses.
- Sample stage.
- Detectors for all signals of interest.
- Display / data output devices.

SEMs always have at least one detector (usually a secondary electron detector), and most have additional detectors. The specific capabilities of a particular instrument are critically dependent on which detectors it accommodates.

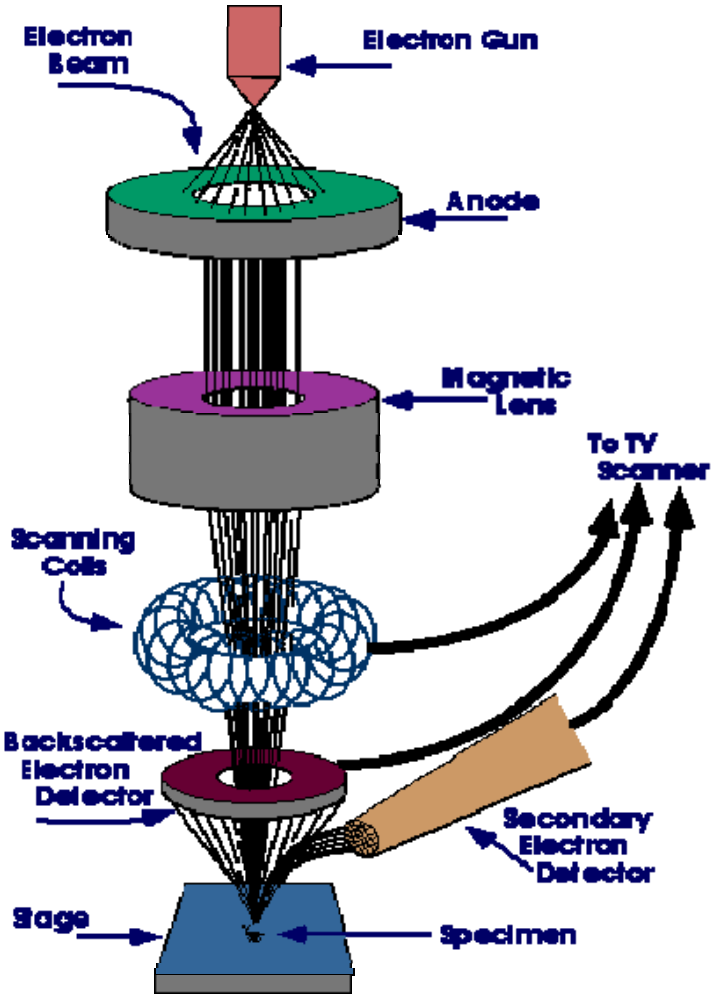

Figure 1.4. Scheme of a scanning electron microscope.

1.12.4. X-ray Energy Dispersive Spectroscopy (EDS).

EDX analysis stands for Energy Dispersive X-ray analysis. Sometimes it is also referred to as EDS or EDAX analysis. It is a chemical microanalysis technique used in conjunction with scanning electron microscope in order to identify composition and provide chemical characterization of a specimen. The EDX analysis system works as

an integrated feature of a scanning electron microscope, and can not operate on its own without the latter.

During EDX analysis, the specimen is bombarded with an electron beam inside the scanning electron microscope. The bombarding electrons collide with the specimen atoms' own electrons, knocking some of them off in the process. A position vacated by an ejected inner shell electron is eventually occupied by a higher-energy electron from an outer shell. To be able to do so, however, the transferring outer electron must give up some of its energy by emitting X-ray, to balance the energy difference between the two electrons' states.

The amount of energy released by the transferring electron depends on from which shell it is transferred, as well as to which shell it is transferred. Furthermore, the atom of every element releases X-rays with unique amounts of energy during the transferring process. Thus, by measuring the amounts of energy present in the X-rays being released by a specimen during electron beam bombardment, the identity of the atom from which the X-ray was emitted can be established.

The output of an EDX analysis is an EDX spectrum (Figure 1.5). The EDX spectrum is just a plot of how frequently an X-ray is received for each energy level. An EDX spectrum normally displays peaks corresponding to the energy levels for which the most X-rays had been received. Each one of these peaks is unique to an atom, and therefore corresponds to a single element. The higher a peak in a spectrum, the more concentrated the element is in the specimen.

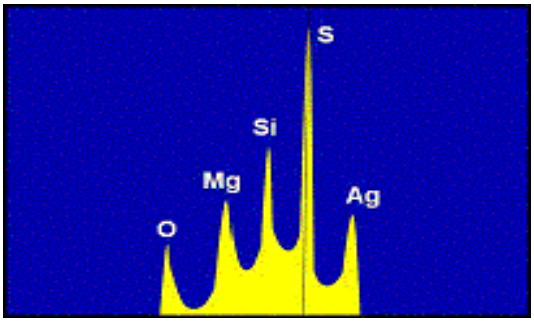

Figure 1.5.Example of an EDX spectrum.

An EDX spectrum plot not only identifies the element corresponding to each of its peaks, but the type of X-ray to which it corresponds as well. For example, a peak corresponding to the amount of energy possessed by X-rays emitted by an electron in the L-shell going down to the K-shell is identified as a K-Alpha peak. The peak corresponding to X-rays emitted by M-shell electrons going to the K-shell is identified as a K-Beta peak, and so on Figure 1.6. [73,74]

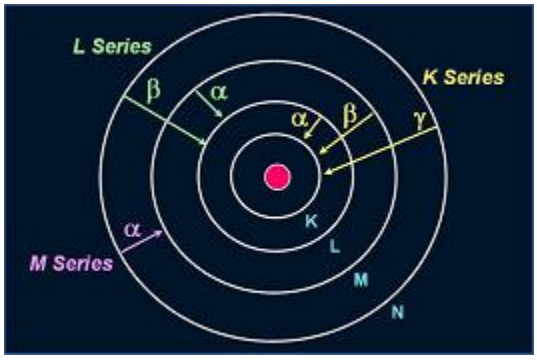

Figure 1.6. Electronic transitions and spectral lines.

1.12.5. Transmission Electron Microscopy (TEM)

Transmission Electron Microscopy is used to identify imperfections in the atomic-level structure of materials by the analysis of microscopic surfaces. A very thin slice of the material to be tested is exposed to a beam of electrons. When the electrons interact with consistent material structure, a constant fraction of electrons is transmitted back from the sample to a detector. Once a structural imperfection is encountered, the fraction of transmitted electrons changes.

Two common methods of TEM microstructural imaging reveal important information about the material being tested. Diffraction contrast is useful in identifying large structures and crystallographic features. Phase contrast is used for high magnification imaging of atomic columns.

Scanned Transmission Electron Microscopy (STEM) is useful for identifying crystal defects and mapping diffracting domains. Electron diffraction analysis can be performed in a variety of modes and provides crystal phase identification, specimen

preferred orientation information, and the determination of crystal lattice constants. Electron diffraction is an important tool employed in crystal defect identification. EELS (Electron Energy-Loss Spectroscopy) utilizes electrons that have lost energy and have their paths slightly and randomly deflected. The amount of energy lost is a function of the specimen's composition. The technique is especially suited to analyzing light elements [73,74].

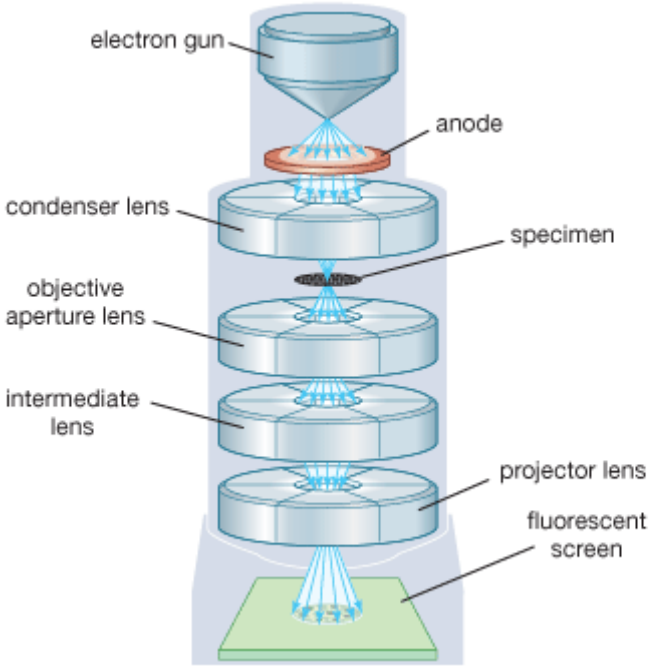

Figure 1.7. Scheme of a transmission electron microscope.

This introduction has addressed the subject of the general procedure for sol-gel synthesis and foundation of the technique briefly and simply to make a summary of the origins and recent developments. It has also made reference to the theoretical introduction of the analytical techniques used in the development of this experimental work.

From the reading of this introduction, it is easy to understand that the coupling of Sonogel-Carbon devices and nanomaterials can be a powerful combination to

obtain new amperometric sensors for the determination of chemical species. At this point, my research work begins.

2. Materials and Methods

2.1. Materials

The materials used in the experimental part of this work are:

- For voltammetric measurements, electrochemical cells of 25 mL were used. BIOHIT (10-100 µL, 20-200 µL and 200-1000 µL) automatic adjustable pipettes were used for additions of solutions in the measuring cell; to take the necessary quantities of precursors in the manufacture of sonosols, and to prepare buffer solutions, 5 µL microsyringe was also employed for additions of solutions in the measuring cell and incorporation of nanoparticles on the Sonogel electrode surface.
- During the experimental work, diverse glass material was used: pipettes, beakers, flasks of different volumes, test tubes, cuvettes, etc…
- Glass capillary tubes were used as the bodies for the composite electrodes: 1.15 mm of internal diameter, 1.55 mm of external diameter, and 70 mm in length.
- To establish electrical contact between electrodes and the potenciostat /galvanostat, we used copper wires of diameter 0.5 mm.
- In the polishing stage of the electrodes, sandpaper (Waterproof Silicon Carbide Paper) fine-grained P # 1200 Struers was used.

Reagents

Species	purity	Commercial House
Sodium citrate	99.5%	Scharlau
Hydrogen tetrachloroaurate(lll)	----	ACROS ORGANICS
Ascorbic acid	99%	Sigma-Aldrich
Pottasium hexacyanoferrate(ll)	99.5%	Fluka
Hydrochloric acid	32%	MERCK
Methyltrimethoxysilane	p.s.	MERCK
Sulphuric acid	96%	MERCK
Di-pottasium hydrogenorthophosphate	99%	Fluka
Pottasium dihydrogenorthophosphate	99.5%	Fluka
Nitric acid	65% QP	Panreac
Graphite	spectroscopic grade	GmbH
Absolute Ethanol	p.a.	MERCK

- The nitrogen used for getting inert atmospheres and deaerating solutions in the measuring cell was N-55 type.

Preparation of solutions.

The description of the procedures for the preparation of solutions is summarized as follows:

- Solution of HCl

For obtaining different synthesized sonosols it was necessary to prepare a solution of HCl 0.2 M. To prepare 100 ml, take 1.966 ml of HCl 32% and make up to the corresponding volume in a volumetric flask.

- Phosphate Buffer Solution(PBS):

To prepare one litre, 34.83 g of di-pottasium hydrogen orthophosphate, and 27.22 g of pottasium dihydrogen orthophosphate were dissolved in 1 litre flask with bi-distilled water.

- Solution of Aqua Regia:

9 mL of concentrated hydrochloric acid was poured into a 25 mL graduated cylinder, carefully and slowly 3 mL of concentrated HNO_3 (nitric acid), were added to prepare the aqua regia. This solution were used to clean glasswares, afterwards the glasswares were washed thoroughly with bi-distilled water, and dried prior to use.

- Solution of ascorbic acid:

1 mM solution of ascorbic acid was prepared by dissolving 2.20 g in 25 mL of bi-distilled water.

- Solution of pottasium hexacyanoferrate(ll)

1 mM of pottasium hexacyanoferrate(ll) solution was prepared by dissolving 5.30 g in 25 mL of bi-distilled water.

Instruments

For performing the experimental work the following instruments were used:

- The synthesis of the Sonogel-Carbon material for the electrodes, as well as of one type of the gold nanoparticles was carried out sonicating with a high power ultrasonic generator, SONICATOR 3000, from MISONIX (MISONIX, Inc. Farmingdale, NY, USA) (equipped with a 13-mm titanium tip), that provides a maximum output power of 600 W.

- UV-Visible measurements were made using a Jasco V-550 (Easton, Maryland, USA) UV-visible spectrophotometer, jasco 32 software connected to a personal computer.

- Transmission electron microscopy (TEM) studies were performed on a JEOL, JEOL JEM-2011 (Jeol, Tokyo, Japan) microscope, operating at 200 KV, equipped with a thermoionic gun (LaB6), a fast change and cold double-gradient sampler.

- Optical microscopy studies were carried out using a NIKON SMZ800 (Nikon, Tokyo, Japan) stereo zoom microscope with table stand and 10x wide field eyepieces. The microscope has a continuous zoom range magnification from 10x to 63x.

- Scanning electron microscopy (SEM) studies were carried out on a QUANTA 200 (FEI Company, Hillsboro, Oregon, USA), normally operating at 20 keV and equipped with a Microanalyzer (EDAX) to perform energy dispersive spectroscopy (EDS).

- The voltammetric measures were made on a potentiostat/galvanostat Autolab® PGSTAT20 of Ecochemie connected to a personal computer and a 663 Metrohm VA Stand module. This module offers Teflon platform with three holes in which the working electrode, reference electrode (Ag/AgCl) and auxiliary electrode (counter electrode) (platinum rod) are inserted. The computer controls the operation carried out in the module by GPES (General Purpose Electrochemical System) program version 4.9. This software performs functions including the generation of signals, data acquisition and processing and storage of the data.
- The pH measurements were performed on a digital pH meter Crison Micro pH 2002 with built-in temperature sensor.
- The agitation of the solutions was carried out using a magnetic stirrer Selecta Agimatic-E.
- The various substances used were weighed on a Mettler AE420 analytical balance model of two fields (40 gr., detection up to 0.01 mg, and 200 gr., detection up to 0.1 mg).
- Milli-Q system (Millipore, Bedford,MA) with a resistance of 18 $M\Omega \cdot cm^{-1}$, was used for obtaining nanopure water by passing two-times distilled water through the system.
- An ultrasonic bath from Selecta was also employed when necessary.

2.2. Methods

Classical synthesis of gold nanoparticles (SN 1)

In a 25 mL Erlenmeyer flask, 20 mL of $HAuCl_4$ 1.31 mM was brought to boil with vigorous stirring on a magnetic stirring hot-plate. Then 2 mL of $Na_3C_6H_5O_7.2H_2O$ 38.8 mM was added to the solution immediately, with vigorous stirring. The yellow $HAuCl_4$ solution changed to dark red within few minutes. Stirring and boiling was continued for about 10 minutes after the observation of the colour change.

The solution was removed from heat and allowed to cool at room temperature. The colloidal solutions were stored in darkness in a clean plastic container in refrigerator prior to use.

Ultrasonic synthesis of gold nanoparticles (SN 2)

In a vial, 1.25 mL of $HAuCl_4$ 1.31 mM solution was vigorous mixed with a high power ultrasound sonicator for 4 minutes. Then 250 µL of $Na_3C_6H_5O_7.2H_2O$ 38.8 mM was added and the insonation process was continued till a dark red colour is obtained (total time of synthesis = 5.5 min) [75,76] The solution was removed and allowed to cool at room temperature before being transfered to a covered plastic container and kept in darkness in refrigerator prior to use.

Preparation of the Sonogel-Carbon electrodes

In summary, the Sonogel-Carbon material for the composite electrodes is prepared in a glass container (5.5 cm high and 1.7 cm in diameter) and the following precursors are added in the order given: 50 µL of HCl solution concentration 0.2 M necessary and 250 µL of MTMOS. Then, the container is placed under the probe transducer, as shown in Figure 2.1, and insonation is carried out for five seconds. A single homogeneous phase which is the sol (start of the hydrolysis) is obtained in this way. Then, 0.25 g of graphite powder is added and homogenized in the mix.

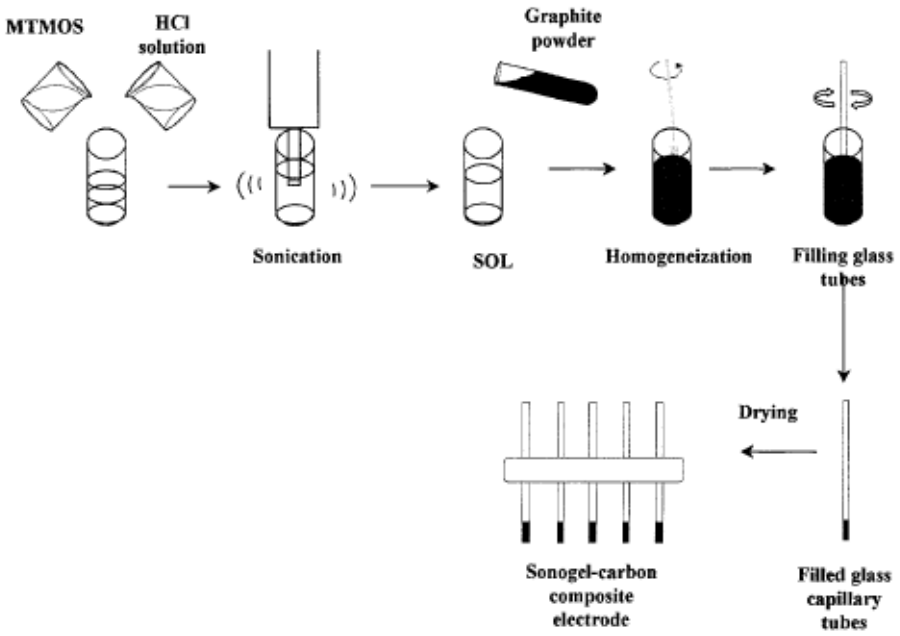

Figure 2.1: Scheme of the steps followed for the fabrication of the Sonogel-Carbon composite electrodes.

With regard to the filling of the capillaries, this operation is performed reproducibly and accurately, avoiding gaps that can remain, what is relatively complicated, taking into account the high viscosity and low external diameter of the capillary. The filling is done by inserting the capillary into the bosom of the vial of synthesis containing sonosol. It has been observed that it is very effective to rotate the capillary in both directions with respect to the vertical axis, while the insertion is done into the sonosol, thus simplifying greatly the operation [12].

Once the capillaries are filled, next step consists of the compression of the material inside the capillary tube, for which a copper wire is used to press on the filling, with the help of a watch glass, where the capillary is supported to prevent the exit of the sonosol from it. Once compacted, the watch glass is removed and, with the help of the same copper wire, the pressure is maintained until a small amount of sonosol falls outside the capillary, thus facilitating subsequent grinding and polishing. Finally they are dried at lab environment for a period ranging between 24 and 48 hours.

Before measurements, the material protruding from the capillary is removed. This is done by using a fine grit sandpaper P#1200, and rubbing, the resulting surface with a glossy paper placed on a flat surface. Thus, we get a smooth and shiny surface.

Electrochemical preparation of Sonogel-Carbon electrodes.

Prior to the deposition of gold nanoparticles on the electrodes, these were electrochemically pre-treated. The electrodes were polarised in sulphuric acid 0.05 M from -0.5 to +1.5 V for 5 cycles and at 0.05 $V \cdot s^{-1}$ (50 $mV \cdot s^{-1}$) of scan rate. Electrodes with similar current backgrounds were selected, carefully washed with Milli-Q water and dried at room temperature before use.

Preparation of the gold nanoparticles modified sensors.

The required amount (3 µL or 5 µL, depending on the case) of gold nanoparticles prepared as described above from the two syntheses, were deposited on the electrodes surface of the appropriate Sonogel-Carbon electrodes and allowed to dry at room temperature in darkness for 24 hours or more. After the drying, the electrodes were stored at $4^{o}C$ in darkness before and after their use. The gold nanoparticles were well adhered to the surface of the electrodes.

3. Results and discussion

3.1. UV-visible spectra of gold nanoparticles: stability studies.

Some previous researches have reported UV–vis spectrophotometry as an effective method to monitor the evolution of metal species in the synthesis of metal particles [77,78]. Thus, in our case, the formation of gold nanoparticles was followed by measuring the absorption of the solution containing gold nanoparticles in the range 200-800 nm using UV-vis spectroscopy. Uv-vis spectra were recorded at room temperature for the nanoparticles from the two synthetic routes.

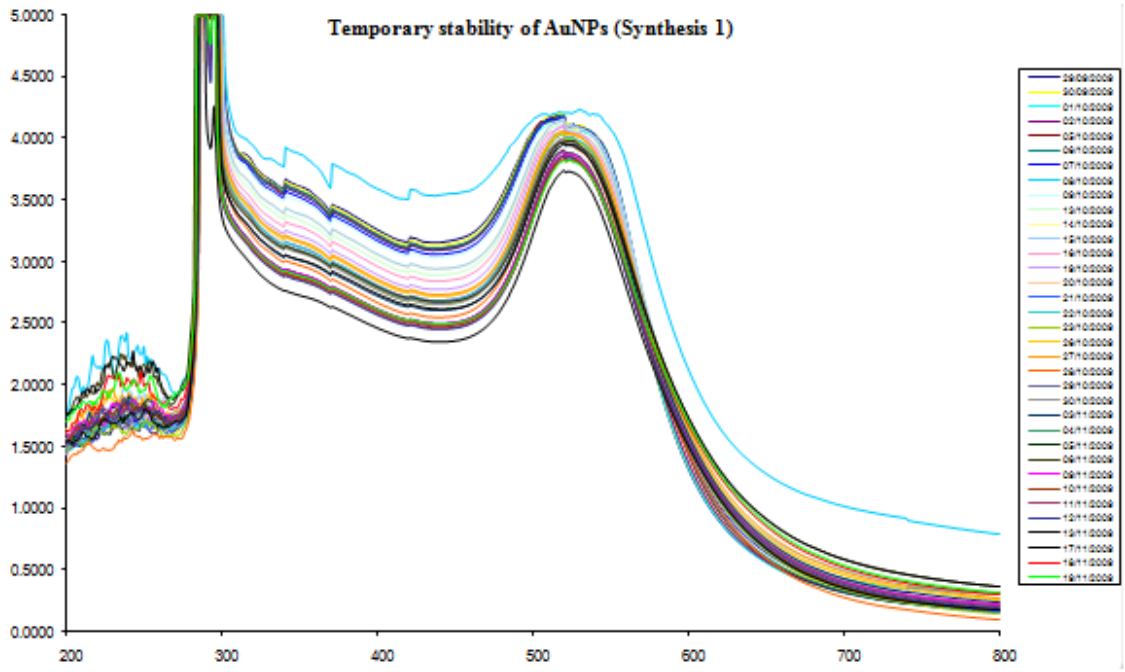

Figure 3.1. UV-vis spectra recorded for gold nanoparticles from synthesis 1

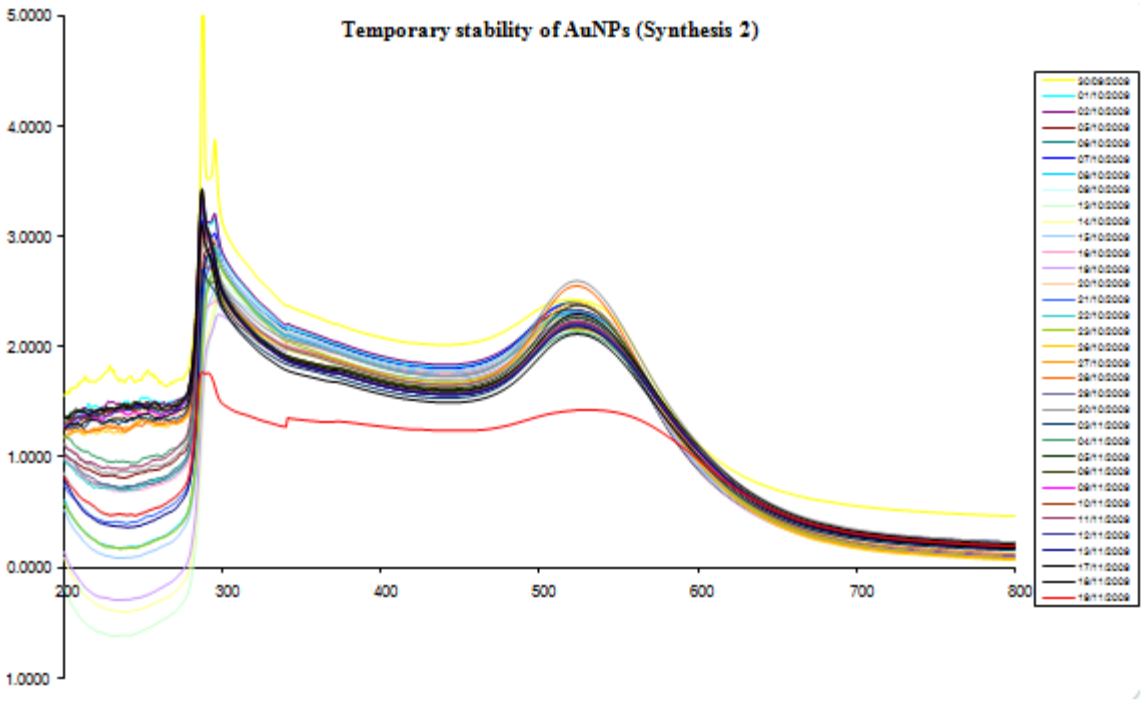

Figure 3.2. UV-vis spectra recorded for gold nanoparticles from synthesis 2

Figures show the UV-vis absorption spectra of the gold nanoparticles. The reduction of Au^{3+} to Au^{0} showed strong absorption peaks that remained near to 525 nm after 30 days for both syntheses 1 and 2, indicating the formation of gold nanoparticles. Richard [79] reported that surface plasmon resonance of metal gold nanoparticles exhibit ruby red colour and give rise to an absorption band at 510-540 nm. The colloidal Au produced is red owing to the absorption of light by free electron oscillations (the surface plasmon).

On one hand, gold nanoparticles synthesized via ultrasonic method, apart from being stable for more than one month, also were well dispersed in solution and with minimal aggregation. In this way by employing a simple and one step reaction in the presence of sodium citrate we could synthesize gold nanoparticles with more than one month stability, promising its application in related fields. On the other hand, Au nanoparticles from synthesis 1 show higher absorption peaks than those from synthesis 2 at the same wavelength (525 nm). This may be due to the lower performance of the synthesis 2 for obtaining gold nanoparticles. However, the difference in the particle size could be more probably the answer. The intensity of

the spectra corresponding to the resonance scattering, which results from the surface plasmon resonance effect increases with the particle size [80]. Thus, the smaller the size, the lower the intensity of the bands in the spectra.

The gold nanoparticles synthesized are easy of depositing onto the desired solid surface. The importance of the methods described in section 2.2, is that the gold nanoparticles are quite stable in solution and were synthesized by reaction with sodium citrate, since we did not introduce either other reducing or protective reagents in the initial solution.

3.2. Electrochemical characterization.

The electrochemical characterization of the Sonogel-Carbon electrodes with and without gold nanoparticles were conducted with the techniques of cyclic voltammetry (CV) and differential pulse voltammetry (DPV). In order to do that, five electrodes with different configurations were tested: a bare Sonogel-Carbon electrode, two AuNPs(SN1)-modified Sonogel-Carbon electrodes, and two AuNPs(SN2)-modified Sonogel-Carbon electrodes. The last two types of electrodes were built by depositing 3 or 5 µL of the corresponding suspension on the surface of previously pre-treated bare Sonogel-Carbon electrodes.

3.2.1. Cyclic voltammetry (CV).

Cyclic voltammetry studies allow the evaluation of the electrochemical behaviour of the devices (bare and AuNPs(SN1,SN2)-modified Sonogel-Carbon electrodes) both in presence and absence of analyte. The experiments were conducted at five different scan rates (10, 25, 50, 75 and 100 $mV \cdot s^{-1}$), in the potential range from -0.3 to +0.7 V, in the presence of pottasium hexacyanoferrate(II) ($K_4Fe(CN)_6$) 1.00 mM. The background (measurements in the absence of $K_4Fe(CN)_6$) was obtained only at

100 $mV \cdot s^{-1}$. Since the sensitivity of cyclic voltammetry is rather low, it is necessary to use a high concentration of the analyte.

As an example, the CV study of one AuNPs-modified Sonogel-Carbon electrode in phosphate buffer solution (PBS) 0.2 M (pH 6.90) at different scan rates is reported in Figure 3.3.

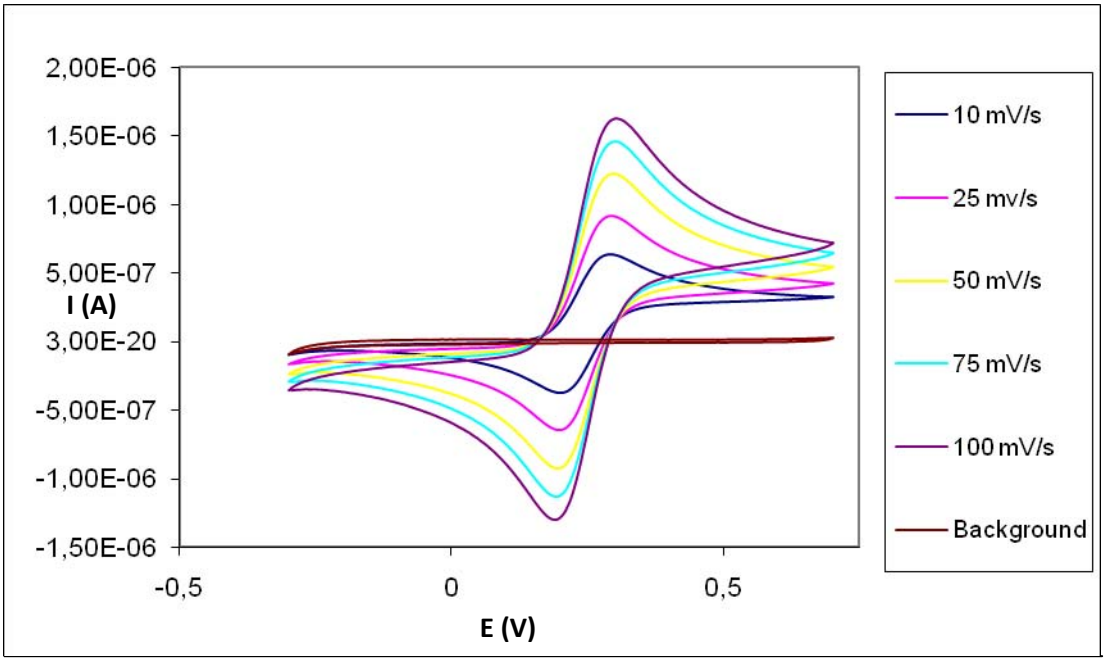

Figure 3.3: Cyclic voltamogramms in phosphate buffer solution 0.2 M (pH 6.9) at various scan rates for the AuNPs(SN2-3 µL)-modified Sonogel-Carbon electrode.

The electrode exhibited a pair of well defined reversible redox peaks at 203 mV and 276 mV, which is attributed to the oxidation/reduction process of iron (Fe) in the analyte: $K_4Fe(CN)_6$. The forward scan potential 276 mV (anodic peak) is related to the oxidation of Fe^{2+} to Fe^{3+}, whereas the reverse potential 203 mV (cathodic peak) is related to reduction of Fe^{3+} to Fe^{2+}. The redox process can be summarized by the next equation:

$$\mathbf{Fe(CN)_6^{4-} \leftrightarrow Fe(CN)_6^{3-} + e^-}$$

Table 3.1.: Electrochemical data for PBS 0.2 M (pH = 6.90), in the presence of $K_4Fe(CN)_6$ 1.00 mM.

E_a (mV)	E_c (mV)	ΔE_p (mV)
276	203	73

The ΔE_p (=E_a - E_c**)** is 73 mV (0.073 V). As it can be seen, the separation of the peak potential values, ΔE_p (=E_a - E_c**)** is greater than 59/n (mV) as expected for a reversible system. There was no redox peak in the absence of $K_4Fe(CN)_6$. As expected, the intensity values of the peaks increased when increasing the scan rate in the presence of the analyte. This may be probably due to the rate of $K_4Fe(CN)_6$ molecule diffussion into the AuNPs-modified Sonogel-Carbon electrode: the higher the scan rate, the higher the current peak.

It should be observed that the anodic and cathodic peak potentials did not shift when increasing scan rates which may be attributed to the reversible nature of the process. Again, this may be rationalised in terms of the equilibrium at the surface of the electrode, which is established so rapidly with fixed peak separations.

Regarding the electrochemical mechanism that takes place on the surface of the electrode, the plots of anodic and cathodic peak currents as a function of the square root of the scan rate (Figure 3.4) show that both parameters were proportional at the scan rates studied (10-100 $mV \cdot s^{-1}$) with determination coefficient of 0.999 at all scan rates, indicating a diffusion-controlled kinetics towards the electrode surface [81-84]. Similar results were obtained for the rest of the Sonogel-Carbon electrodes studied at different configurations. More evidences for the non-adsorptive behaviour of $K_4Fe(CN)_6$ were demonstrated when the sensor was subjected to cyclic voltammetry scans in 0.2 M PBS (pH 6.90), after being used in $K_4Fe(CN)_6$, there was no peak signal at all.

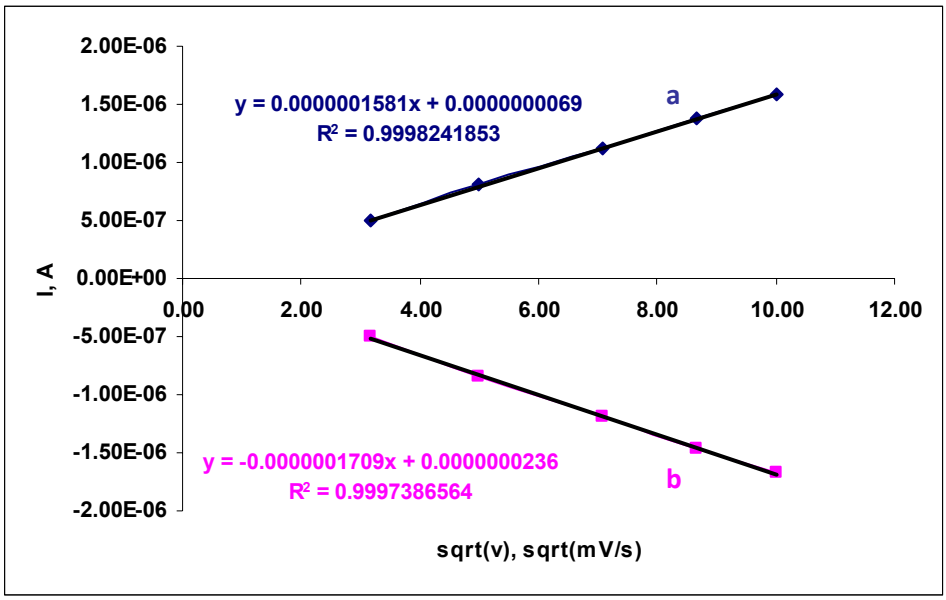

Figure 3.4: Plots of anodic (a) and cathodic (b) peak currents of $K_4Fe(CN)_6$ vs $v^{1/2}$ (square root of the scan rate) from the cyclic voltammograms of Figure 3.3 for AuNPs(SN2-3 µL)-modified Sonogel-Carbon electrode.

The same studies were carried out using AA and hexamine trichlororuthenium(lll) as analyte. However, while for the first one the process was irreversible and very complicated, for the second one the results were not the expected ones, because the mechanism should have corresponded to a reversible process and the experimental results showed that it was irreversible. Deep studies must be done in both aspects for future work.

With respect to the modification of the electrode, as observed in Figure 3.5, the peak intensity is higher for the Sonogel-Carbon electrode modified with gold nanoparticles than for the bare Sonogel-Carbon electrode. This is due to the more electroactive surface of the AuNPs-modified Sonogel-Carbon electrode compared to the unmodified electrode. The presence of AuNPs on the electrode surface increases the superficial area, and thus the electrochemical response versus the analyte ($K_4Fe(CN)_6$).

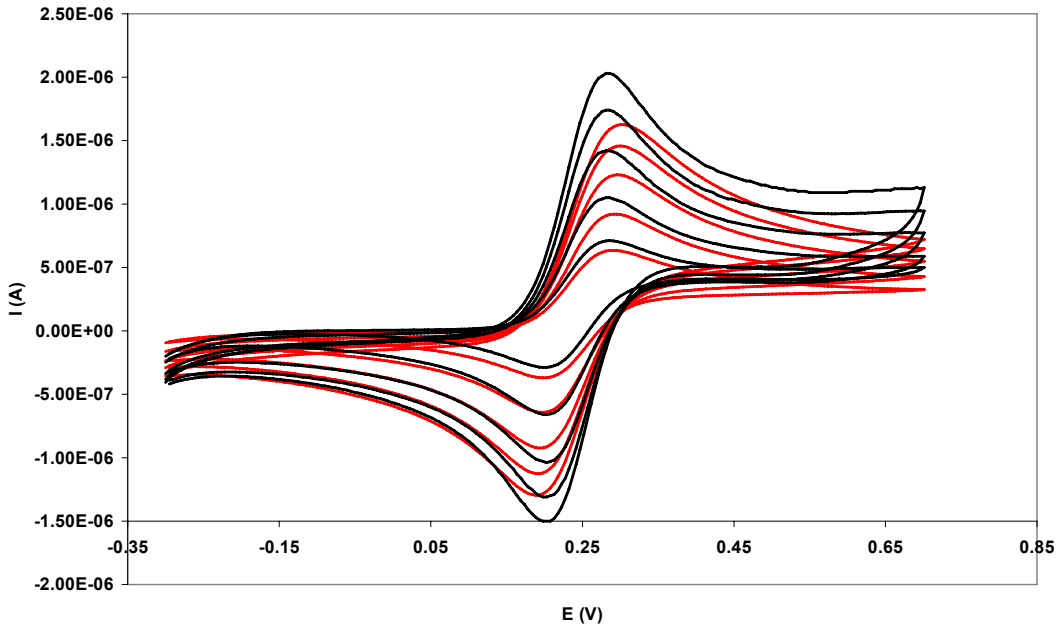

Figure 3.5: Cyclic voltamogramms in phosphate buffer solution 0.2 M (pH 6.9) at different scan rates (10, 25, 50, 75 and 100 mV•s-1), corresponding to a bare Sonogel-Carbon electrode (red) and a AuNPs(SN1-3 µL)-modified Sonogel-Carbon electrode (black).

Furthermore, the peak intensity for the AuNPs (SN1-5 µL)-modified Sonogel-Carbon electrode was higher than that for the same type of electrode but with 3 µL of AuNPs deposited instead of 5, as Figures 3.6 shows. This is obviously owing to an increment in the amount of AuNPs on the electrode surface. That is why the number of electroactive sites also increases, and hence the peak intensity.

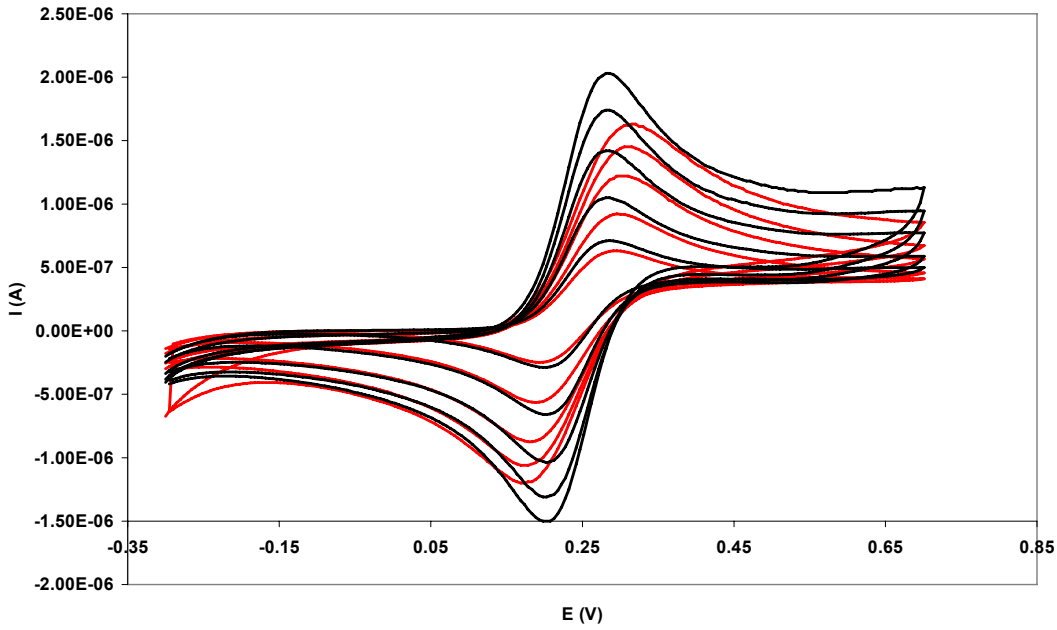

Figure 3.6: Cyclic voltamogramms in phosphate buffer solution 0.2 M (pH 6.9) at different scan rates (10, 25, 50, 75 and 100 mV•s-1), corresponding to a AuNPs(SN1-3 µL)-modified Sonogel-Carbon electrode (red) and a AuNPs(SN1-5 µL)-modified Sonogel-Carbon.

Finally, when comparing two electrodes at the same configuration but modified with AuNPs obtained from different synthetic routes, the results are as follows. From Figure 3.7, the peak intensity of the AuNPs(SN2)-modified Sonogel-Carbon electrode seems lower than the intensity of the AuNPs(SN1)-modified Sonogel-Carbon electrode. This result would indicate that electrodes modified with gold nanoparticles built with the classical (thermal) method of synthesis, performs better than electrodes modified with AuNPs obtained by the ultrasonic synthesis. However, if we have a look to the peak intensity values measured from the CV plots (Table 3.2.), the results are different: the peak intensities are very similar in the two cases. This indicates that the performance of both types of electrodes is comparable. In other words, gold nanoparticles obtained by different synthetic routes show almost the same electrochemical behaviour, despite the differences in the particle size, and thus in the electroactive area. However, these differences are not so high, as the TEM studies will demonstrate in a later section.

Table 3.2.: Peak intensity values for the anodic and the cathodic scans corresponding to a AuNPs(SN2-5 µL)-modified Sonogel-Carbon (SNGC) electrode and a AuNPs(SN1-5 µL)-modified Sonogel-Carbon electrode.

AuNPs(SN2-5 µL)-modified SNGC electrode		AuNPs(SN1-5 µL)-modified SNGC electrode	
I_a (A)	I_c (A)	I_a (A)	I_c (A)
4.91E-07	-4.99E-07	4.97E-07	-4.92E-07
7.34E-07	-7.78E-07	7.76E-07	-7.71E-07
1.02E-06	-1.11E-06	1.06E-06	-1.06E-06
1.24E-06	-1.36E-06	1.24E-06	-1.25E-06
1.43E-06	-1.56E-06	1.34E-06	-1.34E-06

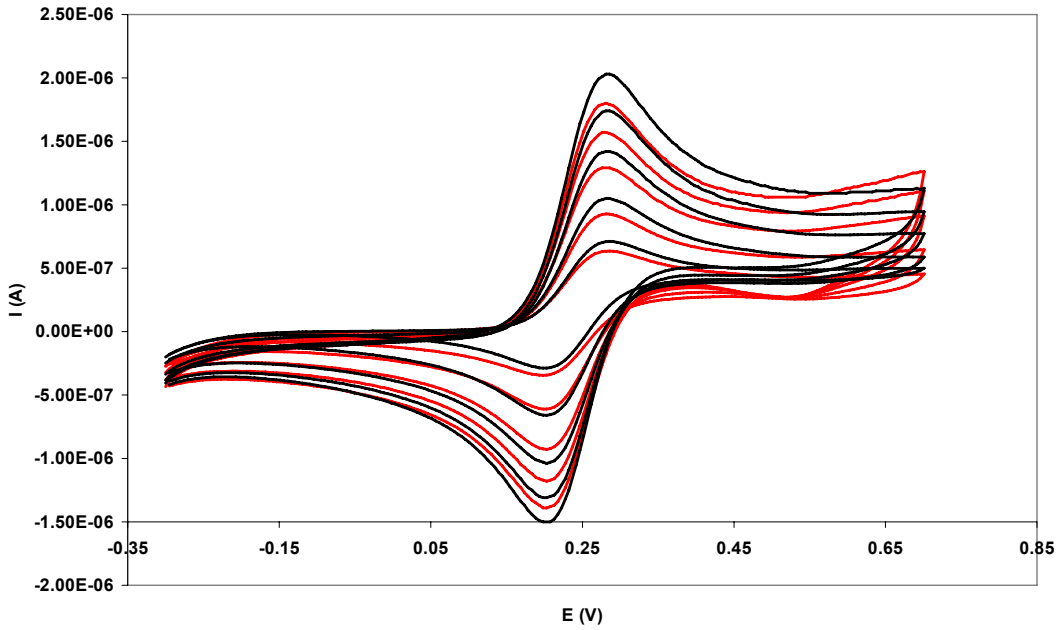

Figure 3.7: Cyclic voltamogramms in phosphate buffer solution 0.2 M (pH 6.9) at different scan rates (10, 25, 50, 75 and 100 mV•s-1), corresponding to a AuNPs(SN2-5 µL)-modified Sonogel-Carbon electrode (red) and a AuNPs(SN1-5 µL)-modified Sonogel-Carbon.

The previous table also corroborates the reversibility of the electrochemical process suffered by the analyte ($K_4Fe(CN)_6$), since the differences between the peak intensities of the anodic and the cathodic signals are minimal.

Relating these results to the synthetic routes, the application of ultrasounds produces nanostructured materials with catalytic activity similar to that corresponding to nanoparticles synthesized by the common and classical method.

To finish with the CV studies, some questions concerning the capacity of the electrodes should be stated. This parameter gives an idea about the amount of charge that is stored in the electrode at a given potential value. It corresponds to the non-faradaic current, *i.e.* the amount of charge that is not used to oxidize or reduce an electroactive species. To evaluate the behaviour of our electrodes, cyclic voltammograms were carried out in phosphate buffer solution 0.2 M at pH 6.9. In our study we have calculated the corresponding values of the experimental observed capacity and the double-layer capacity (Table 3.3). The difference between them is in the form of calculation: on one hand the observed capacity is defined as C_{obs} = i/v, where *i* is the average anodic and cathodic current density and *v* is the scan rate (100 $mV \cdot s^{-1}$); on the other hand, the double-layer capacity consists of the slope of the regression line obtained when representing the average (absolute) values of the anodic and cathodic current densities at different scan rates versus the scan rate values (Figure 3.8). In both cases, those parts of the voltammograms where faradaic intensities (corresponding to oxidation and reduction of the supporting electrolyte) prevailed upon capacitive intensities were not considered.

Table 3.3.: Experimental values of the observed capacity (Cobs) at 100 $mV \bullet s^{-1}$ and the double-layer capacity (C_{dl}) for the different configurations of the Sonogel-Carbon electrodes.

Electrode	C_{obs} ($\mu F/cm^2$) at 100 mV/s	C_{dl} ($\mu F/cm^2$)
Bare SNGC electrode	28	24
AuNPs(SN1-3 µL)-modified SNGC electrode	105	96
AuNPs(SN1-5 µL)-modified SNGC electrode	203	171
AuNPs(SN2-3 µL)-modified SNGC electrode	55	49
AuNPs(SN2-5 µL)-modified SNGC electrode	64	54

As observed in Table 3.3, the lower value for the capacities corresponds to the unmodified SNGC electrode, as expected, since this parameter increases their values because of the presence of chemical species (modifiers) on the surface of the electrodes, gold nanoparticles in our case. The C_{obs} value for the unmodified electrode shows perfect correspondence with previously published results [85]. When depositing nanoparticles on the surface of the Sonogel-Carbon electrodes the capacity values increase: the higher the amount of Au nanoparticles, the greater the capacity values, that is coherent. However, it seems that when modifying SNGC electrodes with Au nanoparticles from synthesis 2, the capacity values are much lower than when using Au nanoparticles from synthesis 1. This means that a AuNPs(SN2)-modified SNGC electrode stores much less amount of charge, and hence much more charge is available to oxidize and/or reduce the analytes. In general, the lower the capacity values, the better the electrochemical performance of the electrodes.

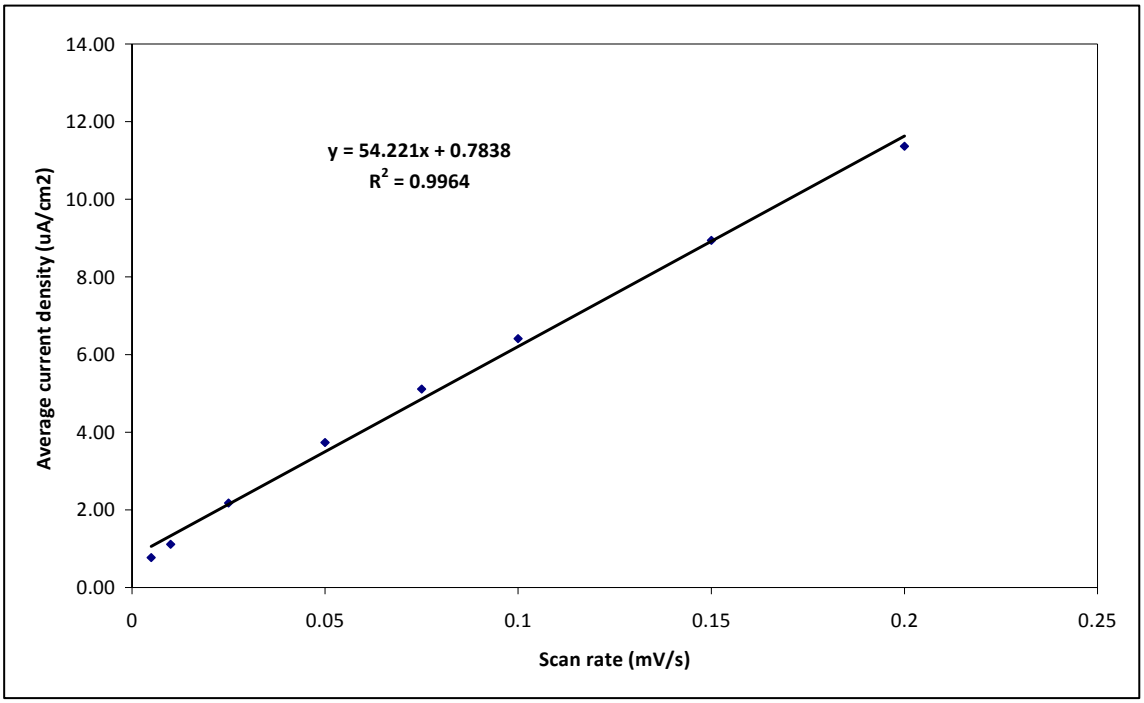

Figure 3.8: Representation of the average (absolute) values of the anodic and cathodic current densities at different scan rates versus the scan rate values in the range from 10 to 200 mV•s-1 for the AuNPs(SN2-5 µL)-modified SNGC electrode.

3.2.2. Differential pulse voltammetry (DPV)

Pulse voltammetry techniques have been established to be very sensitive in the detection of micromolar amounts of ascorbic acid (AA) [86,87]. Thus, Differential Pulse Voltammetry (DPV) has been used to evaluate and demonstrate the good electrochemical performance of our devices when determining this analyte, selected at the beginning as a benchmark.

First of all, the effects of the DPV parameters on the response of the electrodes have been studied by means of three factors and three level Box-Behnken experimental design [88]. These investigations allowed us to individuate the scan parameters leading to optimal sensitivity of the device. The experimental domain studied is described by the quoted Box-Behnken experimental design (see Figure 3.9). The scan parameters to optimize and their corresponding values are summarized as follows: Modulation Amplitude (MA: 10, 50, 100 mV), Step Potential (SP: 4, 8, 16 mV) and Interval Time (IT: 0.2, 0.4, 0.6 s). The optimization process was carried out at 13 different points and at two different concentration values of AA. The results appear in Table 3.4.

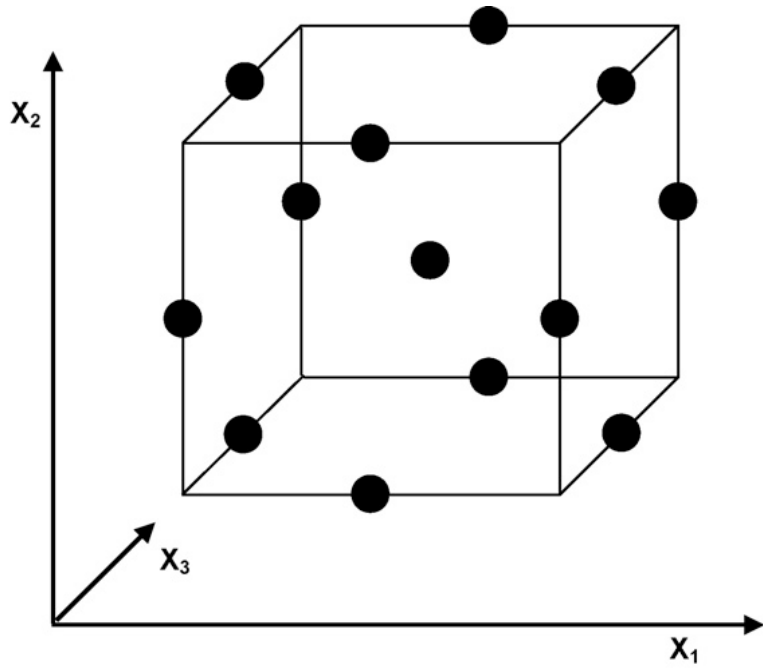

Figure 3.9: Box-Behnken design and sampled points.

Table 3.4: Results of the optimization of the DPV parameters when applying three factors and three level Box-Behnken experimental design.

				[AA] = 0.5 mM		[AA] = 1.0 mM	
Points	**IT (s)**	**SP (mV)**	**MA (mV)**	**I (×10^{-8} A)**	**I/W (×10^{-8} A/mV)**	**I (×10^{-7} A)**	**I/W (×10^{-7} A/mV)**
1	0	-1	-1	6.83	35.00	1.61	8.70
2	0	1	-1	8.71	41.48	2.05	10.78
3	0	-1	1	86.88	434.38	20.15	106.03
4	0	1	1	109.90	499.55	26.09	130.43
5	1	-1	0	40.34	218.03	9.43	55.46
6	1	1	0	50.06	238.38	11.96	64.62
7	-1	-1	0	46.61	233.03	10.97	57.71
8	-1	1	0	58.45	265.66	13.97	66.52
9	1	0	-1	8.22	43.24	1.88	11.05
10	1	0	1	102.95	514.75	24.49	136.06
11	-1	0	-1	9.55	47.73	2.32	13.24
12	-1	0	1	106.15	505.48	25.18	119.88
13	0	0	0	49.78	248.88	11.85	65.83

IT: -1 = 0.2; 0 = 0.4; 1 = 0.6 s
SP: -1 = 4; 0 = 8; 1 = 16 mV
MA: -1 = 0; 0 = 50; 1 = 100 mV

The optimized functions were peak intensity (I) and the ratio of peak intensity and peak width (I/W). In order to select the optimal conditions given by the combination of DPV parameters that offers the highest I and I/W values an analysis of variance (ANOVA) was taken into account. The results are summarized as follows:

- Optimizing I: ANOVA showed that the most significant parameters were SP and MA for both AA concentrations. Moreover, the interaction between

both parameters was also significant. In all cases, the influence of SP, MA and SP*MA on the function I was linear. An example of a regression model at the concentration of AA equal to 0.5 M is:

$$I = 49.775 + 5.809 \cdot SP + 46.572 \cdot MA + 5.285 \cdot SP * MA$$

The goodness of the model is represented by r^2 = 0.9985 and $r_{adjusted}$ = 0.9940, what means a very good fitting. As it can be observed, the DPV parameter that influences more when optimizing I is the modulation amplitude, which possesses the highest regression coefficient in the model.

- Optimizing I/W: when optimizing this other function, ANOVA demonstrate that there is only one significant parameter: MA, for both AA concentrations. Hence, the regression model is constructed only with this DPV parameter and the intercept value. The fitting is also rather good, with r^2 and $r_{adjusted}$ values higher than 0.99.

From this discussion, combinations of DPV parameters corresponding to points 4 and 10 (Table 3.4) gave the highest I and I/W values, which were almost similar for both optimized functions. However, the combination of parameters for point number 4 was chosen as the optimal one because possessed the highest MA and SP values, which were significant parameters according to ANOVA. Thus, the optimal combination of DPV parameters was: IT = 0.4 s, (the medium level of the parameter), SP = 16 mV and MA = 100 mV. Therefore, this combination was chosen for further studies.

In second place and once determined the optimal conditions for the DPV measurements, the next step consisted of obtaining calibration curves for AA at the scan rate of 50 $mV \cdot s^{-1}$. The potential range at which the sensor responses were studied was from -0.5 V to 1.2 V in a 0.2 M buffer solution. For this purpose, several calibration curves for AA were obtained by using the SNGC electrodes at different configurations.

Together with the determination coefficient that give us an idea about the goodness of the regression model, special attention was also paid to the

slope of the regression lines, which represents the sensitivity (measured in A/M) of the sensor for this analyte. The calibration curves were obtained for an AA concentration range from $\sim 1.5\times10^{-6}$ M to $\sim 4.0\times10^{-3}$ M. For each calibration curve, 18 points at different AA concentrations within this range (three orders of magnitude) were measured, with three replicates. This means at least 54 measurements for each electrode.

Figure 3.10 shows one example of the calibration curve obtained for AA when using AuNPs (SN1-5 µL)-modified Sonogel-Carbon electrode.

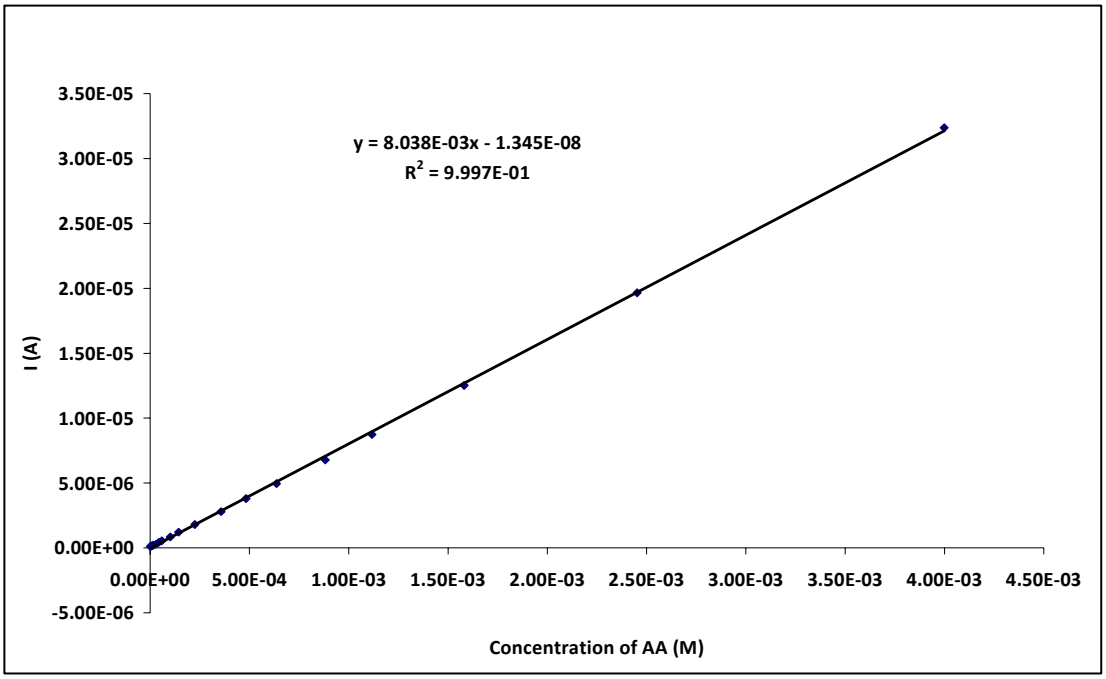

Figure 3.10: Calibration curve for AA using an AuNPs(SN1-5 µL)-modified SNGC electrode.

In Figure 3.11, an example of the DPV voltammograms corresponding to the calibration curve reported in Figure 3.10 for ascorbic acid is shown.

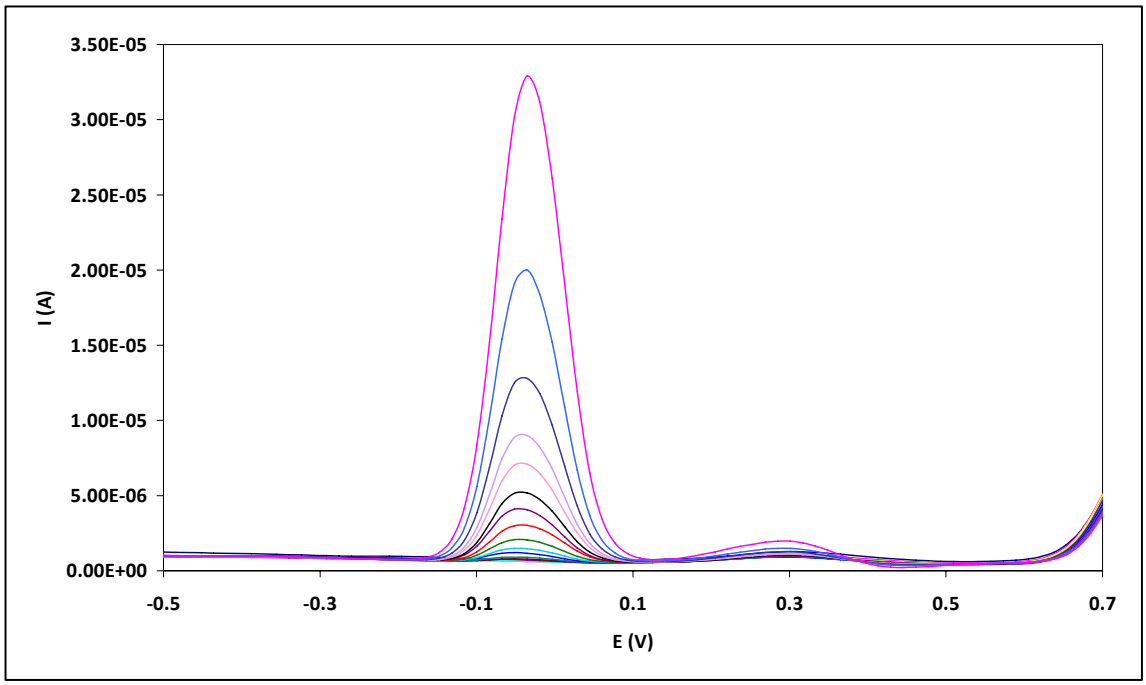

Figure 3.11: DPV voltammograms corresponding to the calibration curve reported in Figure 3.10 for AA; the electrode used was the AuNPs(SN1-5 µL)-modified SNGC electrode.

Table 3.5 shows the best calibration curves obtained for the different types of SNGC used throughout this research work, in terms of slope and determination coefficient values.

Table 3.5: Results of the best calibration curves obtained for AA when using the different types of Sonogel-Carbon electrodes employed.

Electrode	Slope (A/M)	r^2
Bare SNGC electrode	2.314E-03	0.99991
AuNPs(SN1-3 µL)-modified SNGC electrode	5.856E-03	0.99996
AuNPs(SN1-5 µL)-modified SNGC electrode	8.153E-03	0.99979
AuNPs(SN2-3 µL)-modified SNGC electrode	5.727E-03	0.99871
AuNPs(SN2-5 µL)-modified SNGC electrode	6.832E-03	0.99918

As observed, when increasing the amount of nanoparticles deposited on the surface of the electrodes, the sensitivity of the electrochemical device for AA also increases. The performances of the AuNPs(3 µL)-modified Sonogel-Carbon electrodes are similar. However, when depositing the 5 µL of the Au colloidal solution, the results are rather different, giving the AuNPs(SN1-5 µL)-modified SNGC electrode, the best sensitivity. However, it is necessary to remember that this electrode at this configuration showed the highest capacity values when measuring $K_4Fe(CN)_6$. Thus, if one electrode at certain configuration to determine AA or other analyte is wanted to be proposed, it is necessary to achieve a compromise between sensitivity and capacity.

In third place, reproducibility and repeatability studies were developed as well. In the case of the reproducibility studies, several calibration curves for AA were obtained by using three different SNGC electrodes for each one of the configurations tested. The results expressed in terms of the average slope and the respective coefficients of variation are shown in Table 3.6:

Table 3.6: Results obtained for the reproducibility studies by using three different SNGC electrodes for each one of the configurations tested.

Electrode	Average slope (A/M)	CV of slope (%)
Bare SNGC electrode	2.173E-03	12.09
AuNPs(SN1-3 µL)-modified SNGC electrode	5.715E-03	8.57
AuNPs(SN1-5 µL)-modified SNGC electrode	8.396E-03	4.26
AuNPs(SN2-3 µL)-modified SNGC electrode	4.682E-03	1.68
AuNPs(SN2-5 µL)-modified SNGC electrode	6.766E-03	0.86

As it can be seen, the results are coherent with those reported previously in Table 3.5 as the best ones for every electrode. The trend in the slope values is the same. However, in Table 3.6 they represent average values obtained from the calibration

curves corresponding to three different electrodes for each one of the configurations. Nevertheless, regarding the coefficient of variation for the slope, although the results are good in general, excepting perhaps for the first two electrodes, the best results are obtained for the AuNPs(SN2)-modified SNGC electrodes. In other words, the reproducibility is remarkable good in this case. This means that:

1. AuNPs(SN2)-modified SNGC electrodes performs better in terms of reproducibility, despite the high number of measurement that are necessary to be done with only one electrode to obtain a single calibration curve (at least 54; see the discussion for searching the optimal DPV conditions).

2. The process of fabrication of the electrodes is also very reproducible, what is very difficult for modified composite electrodes: a) the Sonogel-Carbon material, and b) the deposition of gold nanoparticles.

3. When trying to propose one configuration for the SNGC electrodes to determine AA or other analyte, as well as taking into account the capacity values and the sensitivity, reproducibility is other important parameter with which a compromise should be achieved.

With respect to the repeatability studies, a SNGC electrode for each configuration was tested and the average slope and the coefficient of variation for the slope for at least two calibration curves using the same electrode were also obtained. The results are reported in Table 3.7.

Table 3.7: Results obtained for the repeatability studies by using independently three different SNGC electrodes for each one of the configurations tested. The number of calibration curves obtained for each electrode was two at least.

Electrode	Average slope (A/M)	CV of slope (%)
Bare SNGC electrode	1.886E-03	0.11
AuNPs(SN1-3 µL)-modified SNGC electrode	5.672E-03	2.07
AuNPs(SN1-5 µL)-modified SNGC electrode	8.581E-03	0.01
AuNPs(SN2-3 µL)-modified SNGC electrode	4.649E-03	1.16
AuNPs(SN2-5 µL)-modified SNGC electrode	5.820E-03	19.02

In this study, the electrode that offered the worst results was the AuNPs(SN2-5 µL)-modified SNGC electrode. It seems that some problem with the deposition took place or perhaps, an unexpected degradation of the electrode surface occurred due to the intensive use of the amperometric sensor. On the contrary, the AuNPs(SN2-3 µL)-modified SNGC electrode showed no problems. As well as sensitivity, capacity, and reproducibility, repeatability should also be taken into consideration to propose one configuration of the SNGC electrodes to determine AA or some other analyte.

Finally, some comments regarding the detection and quantification limits (LD and LQ, respectively) for the electrodes tested at different configurations should be given. Table 3.8 shows the best values obtained for both LD and LQ when using each of the configurations for the SNGC electrodes.

Table 3.8: Best detection and quantification limits obtained for different SNGC electrodes for each one of the configurations tested.

Electrode	LD (M)	LQ (M)
Bare SNGC electrode	1.13E-05	3.78E-05
AuNPs(SN1-3 µL)-modified SNGC electrode	5.26E-06	1.75E-05
AuNPs(SN1-5 µL)-modified SNGC electrode	6.84E-06	2.28E-05
AuNPs(SN2-3 µL)-modified SNGC electrode	3.71E-06	1.24E-05
AuNPs(SN2-5 µL)-modified SNGC electrode	7.24E-06	2.41E-05

LD was calculated as three times the standard deviation of the blank and LQ as ten times this value as reported by Miller and Miller [89]. The lowest LD and LQ values were obtained for the AuNPs(SN2-3 µL)-modified SNGC electrode. Then, the second best LD and LQ values were obtained for the same configuration of electrode, but using AuNP from synthesis 1. Then, electrodes modified with 5 µL of gold nanoparticles give the best values. And finally, the worst values are obtained for the unmodified electrode. This means that gold nanoparticles play an important role in the determination of AA.

Perhaps to get a very low detection limit for ascorbic acid (vitamin C) is not so important, since it is commonly used at higher concentrations as food additive (E300) due to its antioxidant properties.

3.3. Structural characterization.

The structural characterization of the surface of the Sonogel-Carbon electrodes at all the different configurations were carried out by employing several instrumental techniques: optical microscopy (OM), scanning electron microscopy (SEM) and X-ray energy dispersive spectroscopy (EDS). The morphology, shape and size distribution of gold nanoparticles from the two synthetic routes were studied by transmission

electron microscopy (TEM). As in the electrochemical studies, the configurations tested for the electrodes were: a bare Sonogel-Carbon electrode, two AuNPs(SN1)-modified Sonogel-Carbon electrodes, and two AuNPs(SN2)-modified Sonogel-Carbon electrodes. The last two types of electrodes were built by depositing 3 or 5 µL of the corresponding suspension on the surface of previously pre-treated bare Sonogel-Carbon electrodes.

3.3.1. Optical microscopy (OM).

As a first approximation, the surface morphology of the Sonogel-Carbon electrodes at different configurations was analysed by optical microscopy. Figure 3.12 shows the optical microscopic images of the electrode surface after being used. The presence of gold nanoparticles and graphite particles in the matrix is evident.

As observed from the photographs, golden colour in A) and B) indicates the presence of gold nanoparticles and black colour represents graphite. The borders of the electrodes correspond to the glass of the capillary tubes. Some holes and fissures can be also observed on the surfaces, since they have been used and it is normal that the material had suffered from some erosion.

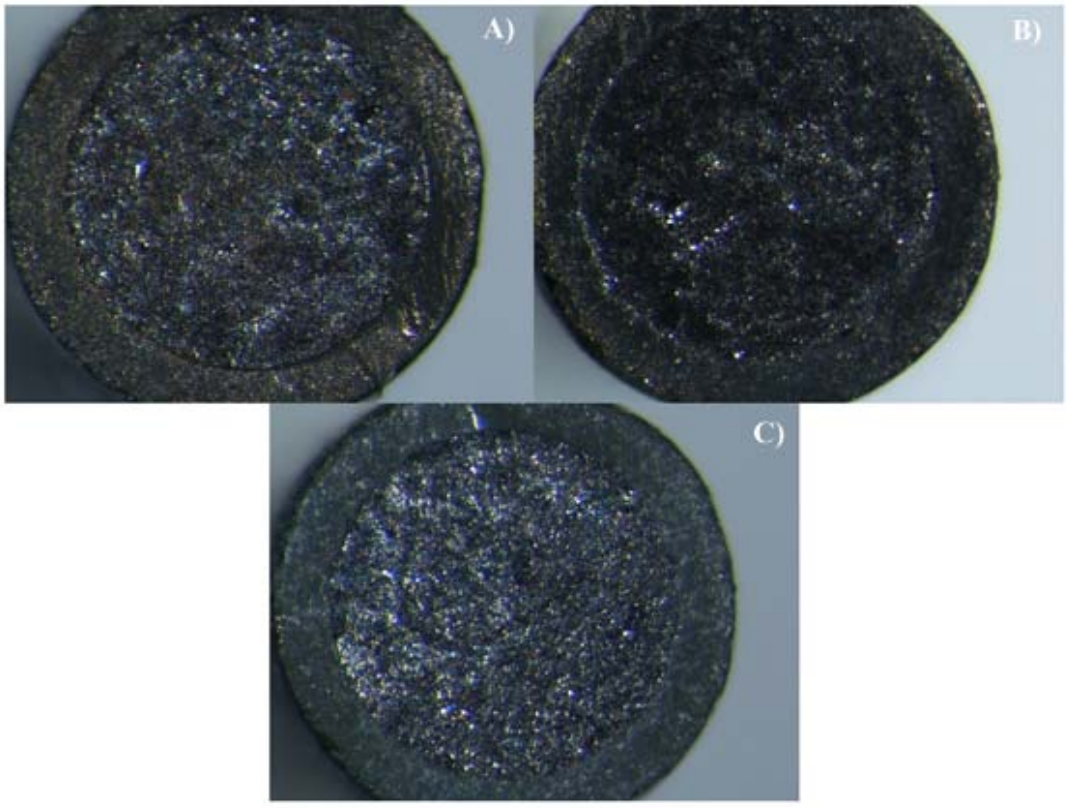

Figure 3.12: Optical microscopy photographs of Sonogel-Carbon electrodes at the magnification 10x: A) AuNPs(SN1-5 µL)-modified SNGC electrode; B) AuNPs(SN2-5 µL)-modified SNGC electrode; C) bare SNGC electrode.

3.3.2. Scanning electron microscopy (SEM) and X-ray energy dispersive spectroscopy (EDS).

The SEM and EDS studies were carried out on several SNGC electrodes at different configurations. The samples were distributed as follows:

1. Bare Sonogel-Carbon electrode.
2. AuNPs(SN1-3 µL)-modified SNGC electrode.
3. AuNPs(SN1-5 µL)-modified SNGC electrode.
4. AuNPs(SN2-3 µL)-modified SNGC electrode.

5. AuNPs(SN2-5 µL)-modified SNGC electrode.

Each sample was duplicated: one for the corresponding electrode used, and other for the electrode not used.

For each sample, the SEM and EDS studies were performed on the same equipment and at the same time, as it was mentioned in the experimental section. As SEM studies were carried out at low vacuum, it was not necessary a previous step of coating the samples with gold. The micrographs were taken at 20 kV in all cases and at different magnifications: 90x, 160x and 600x. Higher magnifications were used to observe some interesting details, mainly when studying the presence of gold nanoparticles on the surface of the electrodes.

- Bare Sonogel-Carbon electrodes (used and not used).

Figure 3.13 shows the SEM micrographs and the EDS spectra corresponding to this electrode at the quoted configuration for two electrodes: one that has been used (Figure 3.13 A) and other that has not been used (Figure 3.13 B).

With respect to the electrode used, the appearance is normal for an electrode that has been used many times, with holes and fissures. However, the erosion is not so remarkable; that is why there is no great separation of the material from the walls of the capillary tube. During the gelification step and the subsequent use, the volume contraction suffered by the electrode has been very low, what is very good for the device. Moreover, there are some fractures that show certain directionality; they can be attributed to the polished step of the electrode.

When comparing with the electrode not used, the same low volume contraction and erosion is observed. Fissures with certain directionality appear as well, what confirms that they have been originated during the polished step. The smaller number of holes and fissures that appear here with respect to the electrode used, correspond to the erosion occurred during the electrochemical polarisation or activation of the Sonogel-Carbon electrodes.

The EDS spectra are identical and confirm only the presence of Si, O and C: the first two ones corresponding to the Sonogel matrix and C as the massive modifier.

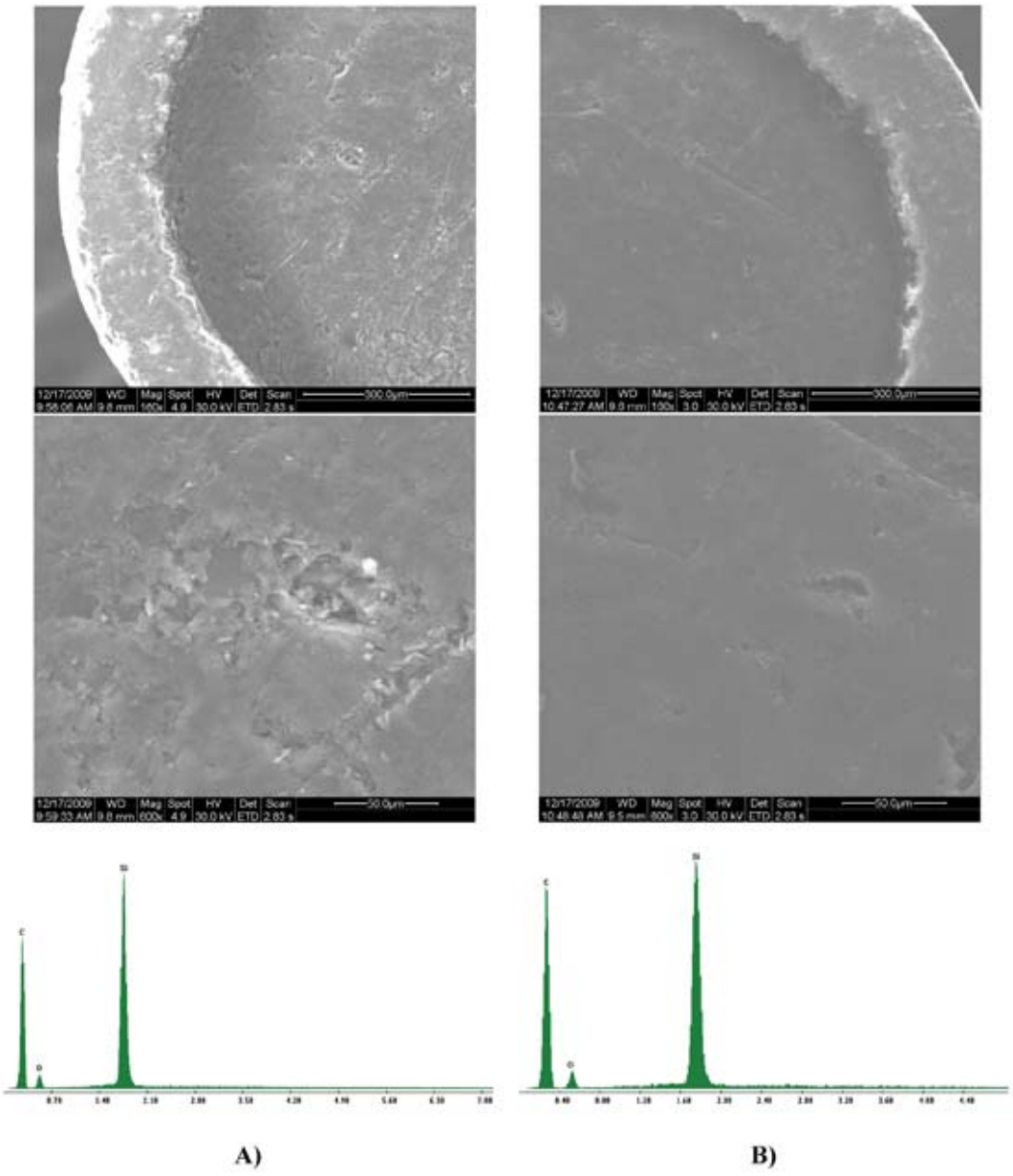

Figure 3.13: SEM micrographs and the EDS spectra corresponding to the bare SNGC electrode: A) used and B) not used.

- AuNPs(SN1-3 µL)-modified SNGC electrode.

Figure 3.14 shows the SEM micrographs and the EDS spectra corresponding to this type of electrode: one used (Figure 3.14 A) and other not used (Figure 3.14 B).

When looking at the micrographs for the AuNPs-modified SNGC electrode used, the typical erosion in the form of holes and fissure due to its utilization can be observed.

As happened with the bare electrodes, the volume contraction and the subsequent separation of the composite material from the capillary tubes is almost inexistent. When increasing the magnification, a great number of particles, in the form of aggregates appear on the sensor surface, which corresponds to gold nanoparticles (from synthesis 1 in this case). The presence of Au is corroborated by the EDS spectrum: one peak related to the K-alpha at ~2.0 eV and two peaks for the K-beta at ~10.0 and ~12.0 eV, respectively. The intensity of these peaks increase dramatically when focusing the electron beam on the particles.

The same comments done previously regarding the erosion and the volume contraction can be done here. Some holes and fissures continue appearing due to the electrochemical polarisation of the electrode. Remember that during this procedure, the electrode is put into a H_2SO_4 0.05 M solution (pH $\simeq$ 1). In previous studies, it was observed that very acid pH values caused great erosion on the Sonogel-Carbon electrode surface. At higher magnifications several types of particles can be detected: some of them similar to those found in the electrode used and others showing shapes similar to a 'bacteria'. In both cases, and thanks to the EDS spectra, Au is found there together with Na, K and Cl. Cl comes from the Sonogel synthesis (acid catalyst), K from the buffer used to clean the electrode surface after the polarisation and Na from the Au colloidal solution (reducing and protective reagent). Cl does not appear always coming from the synthesis of the SNGC electrodes. Only in several occasions its presence has been corroborated on the electrode surface by SEM-EDS.

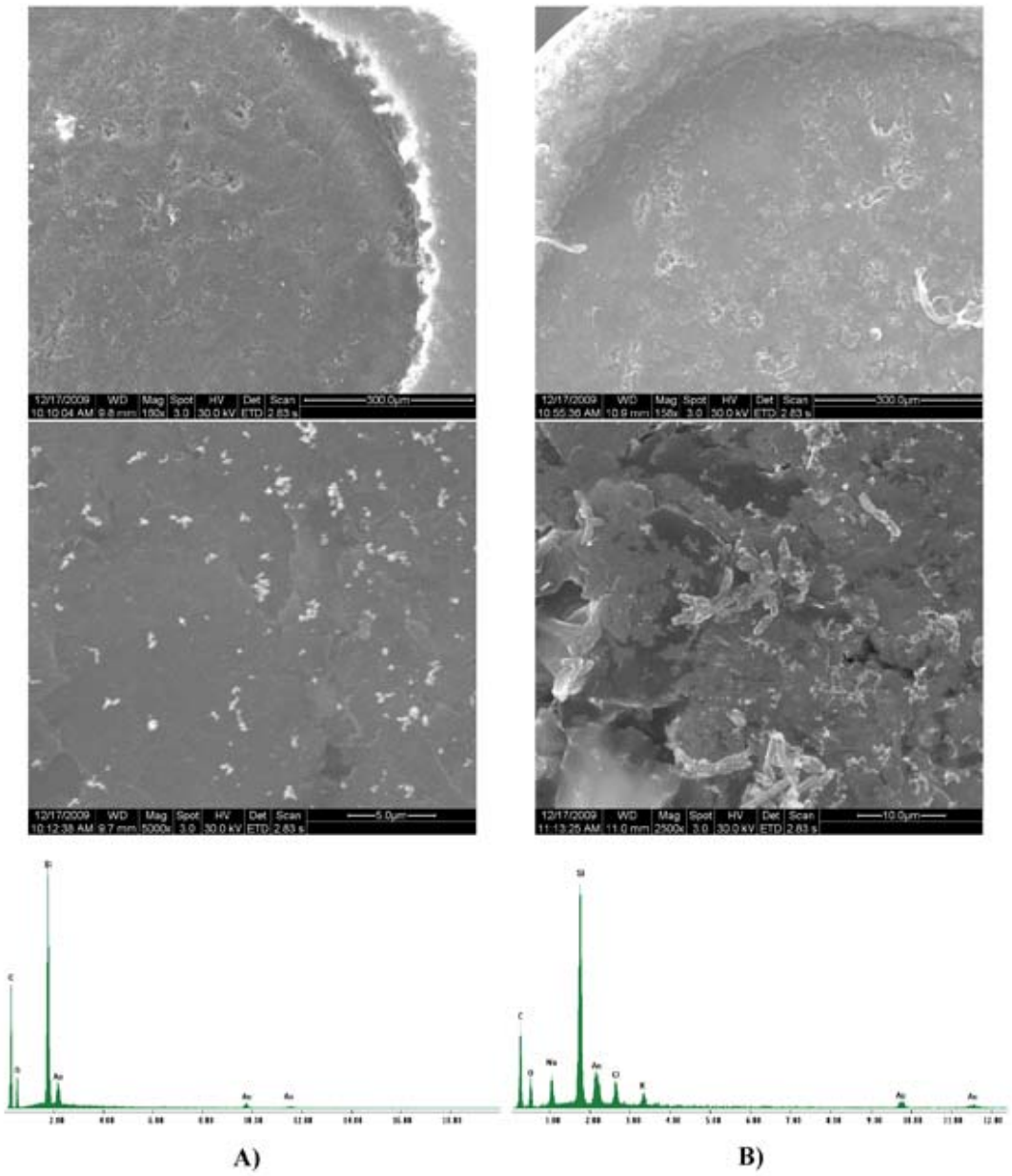

Figure 3.14: SEM micrographs and the EDS spectra corresponding to the AuNPs(SN1-3 µL)-modified SNGC electrode: A) used and B) not used.

- AuNPs(SN1-5 µL)-modified SNGC electrode.

Figure 3.15 shows the SEM micrographs and the EDS spectra corresponding to this type of electrode: used (Figure 3.15 A) and not used (Figure 3.15 B).

For this type of electrode, the same comments regarding holes, fissures, volume contraction and erosion, in general, can be used. At higher magnifications it is also possible to observe particles corresponding to gold nanoparticles. In the case of the electrode not used, the like-bacteria particles appear as well, and its corresponding EDS spectrum also shows the presence of Na, K and Cl. However, from the images it is clear that the amount of nanoparticles is higher for AuNPs(5 µL)-modified SNGC electrodes than for AuNPs(3 µL)-modified SNGC electrodes, what is coherent. The crystalline forms that appear on the surface of the electrode not used seem to be NaCl and KCl crystals surrounded by AuNPs, according to the EDS spectrum when focusing the electron beam on them. The origin of the different ions has been explained previously.

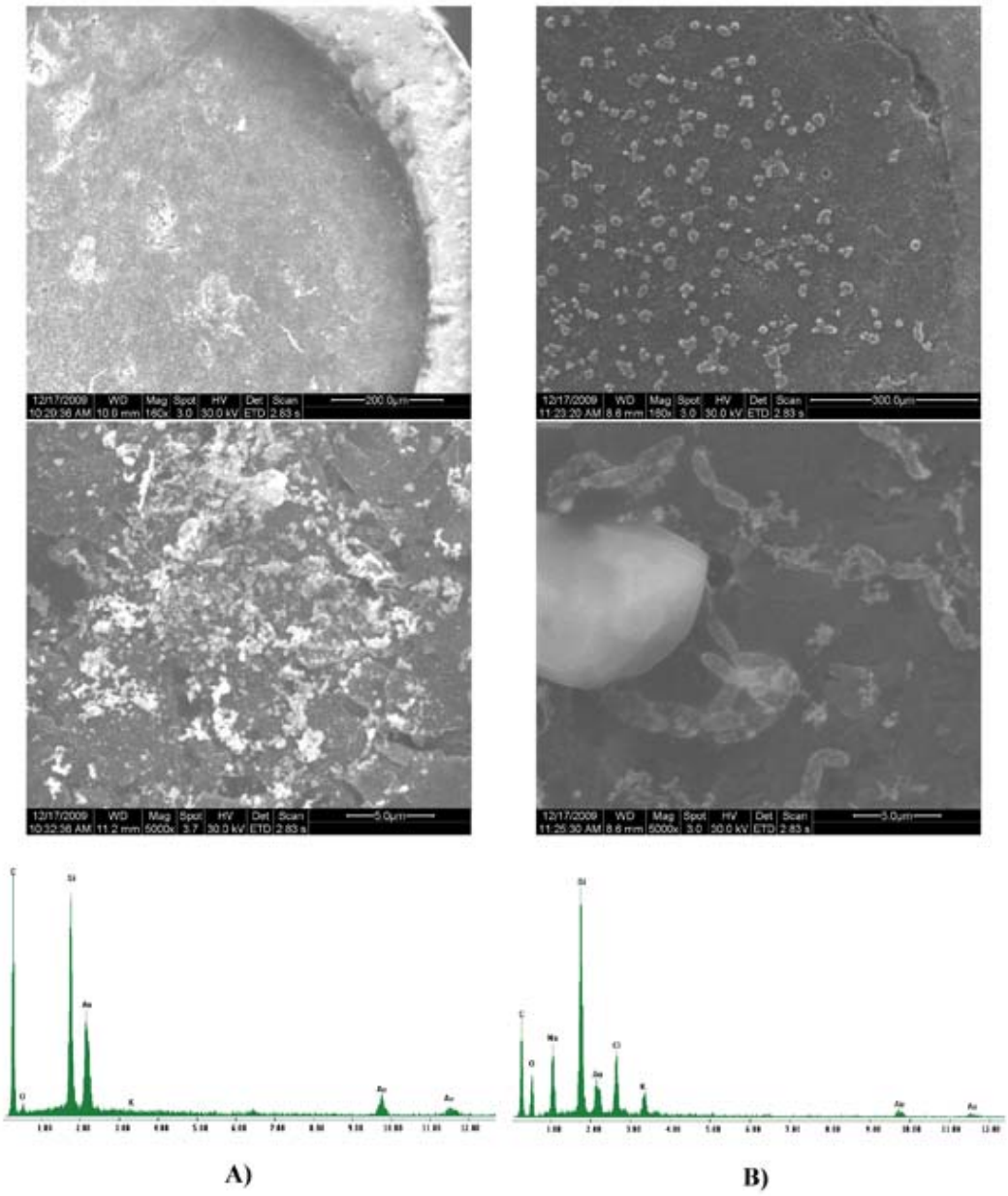

Figure 3.15: SEM micrographs and the EDS spectra corresponding to the AuNPs(SN1-5 µL)-modified SNGC electrode: A) used and B) not used.

- AuNPs(SN2-3 µL)-modified SNGC electrode.

Figure 3.16 shows the SEM micrographs and the EDS spectra corresponding to this type of electrode: one used (Figure 3.16 A) and other not used (Figure 3.16 B). These electrodes have been modified with gold nanoparticles synthesized by the ultrasonic method (SN2) and not by the thermal method (SN1) like in the last two cases. Moreover, the second micrograph corresponding to the electrode used (A)

has been taken with a different detector: instead of a secondary electron detector (the most commonly used), a backscattered electron detector was employed. Hence, it is easier to identify different phases based on qualitative chemical analysis, especially when there is much difference in the atomic number, *i.e.* SNGC matrix and gold nanoparticles.

According to this, from the Figure 3.16 A, it is very simple to distinguish gold nanoparticles from the SNGC matrix and how those coat the electrode surface. The presence of the AuNPs is also corroborated by the EDS spetrum. The microanalysis technique also gives information about some impurities: Cl, K, P and Na coming from the SNGC synthesis, the buffer and the Au colloidal solution. The electrodes offer the same aspect regarding the erosion problem as well. In the case of the electrode not used, it has been necessary to use a very higher magnification to observe the gold nanoparticles; that is why the image of the micrograph is a bit astigmatic. The like-clouds shapes in light-grey correspond to aggregates of gold nanoparticles.

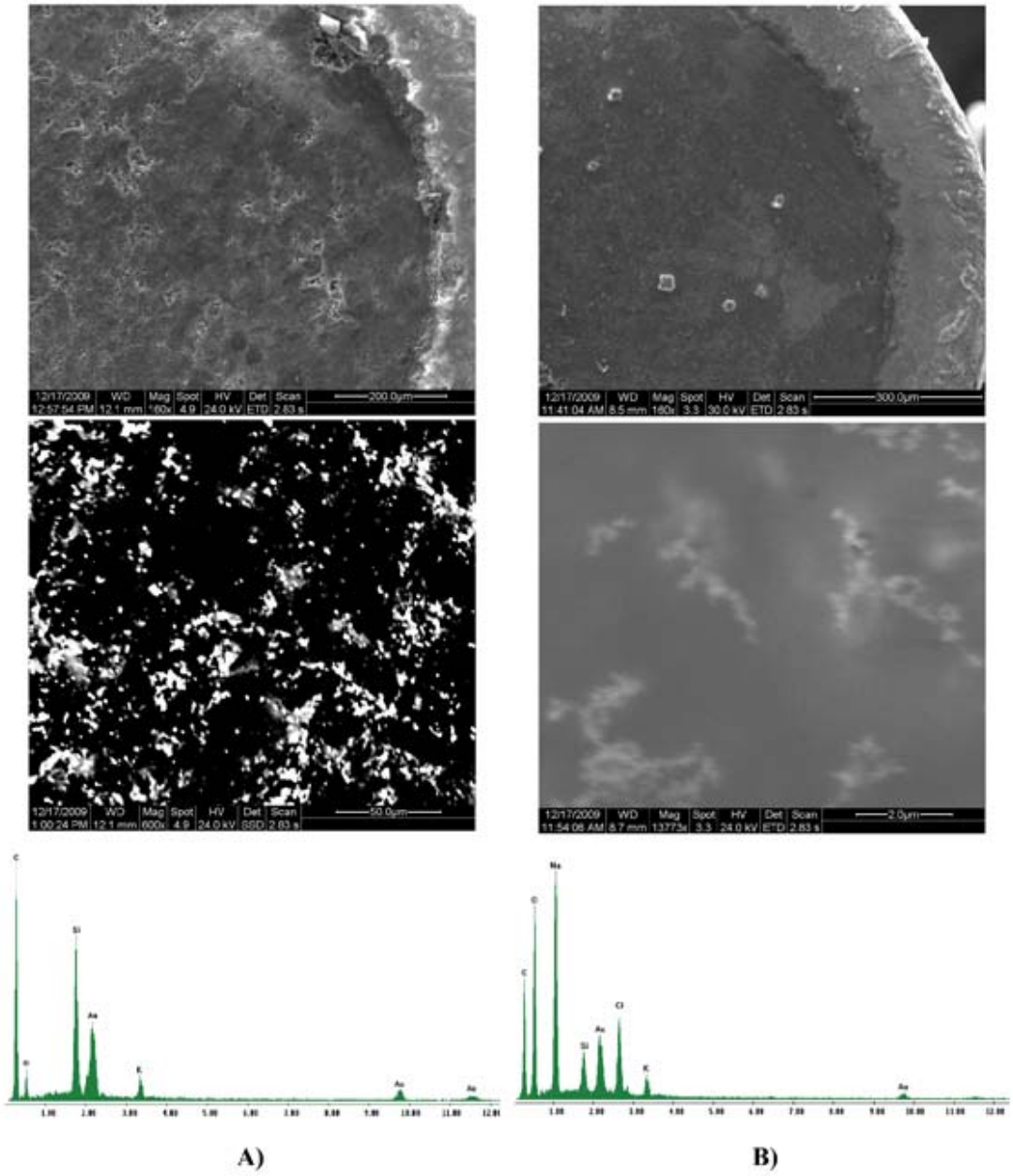

Figure 3.16: SEM micrographs and the EDS spectra corresponding to the AuNPs(SN2-3 µL)-modified SNGC electrode: A) used and B) not used.

- AuNPs(SN2-5 µL)-modified SNGC electrode.

Finally, Figure 3.17 shows the SEM micrographs and the EDS spectra corresponding to this type of electrode: used (Figure 3.17 A) and not used (Figure 3.17 B). For the electrode not used, a backscattered detector has also been utilized. That is why the

micrographs show such good contrast between the SNGC matrix and the particles on the electrode surface.

The micrographs corresponding to the electrode used perhaps are not so good. In this case, it seems that the electrode has not been cleaned adequately; that is why the surface appears covered by a thin film of the phosphate buffer solution. The EDS spectrum offers a very intense K-alpha band for Au, as well as the corresponding ones to Na and K. Owing to the presence of this film, erosion on the electrode surface is not able to be detected. When looking at the micrographs of the electrode not used, the situation is the same; however, here it is easier to detect star-shaped crystals also corresponding to the buffer. Thanks to the use of the backscattered detector and the absence of the thin film of buffer, the existence of gold nanoparticles can be evidenced directly at higher magnifications, corroborated by the microanalysis.

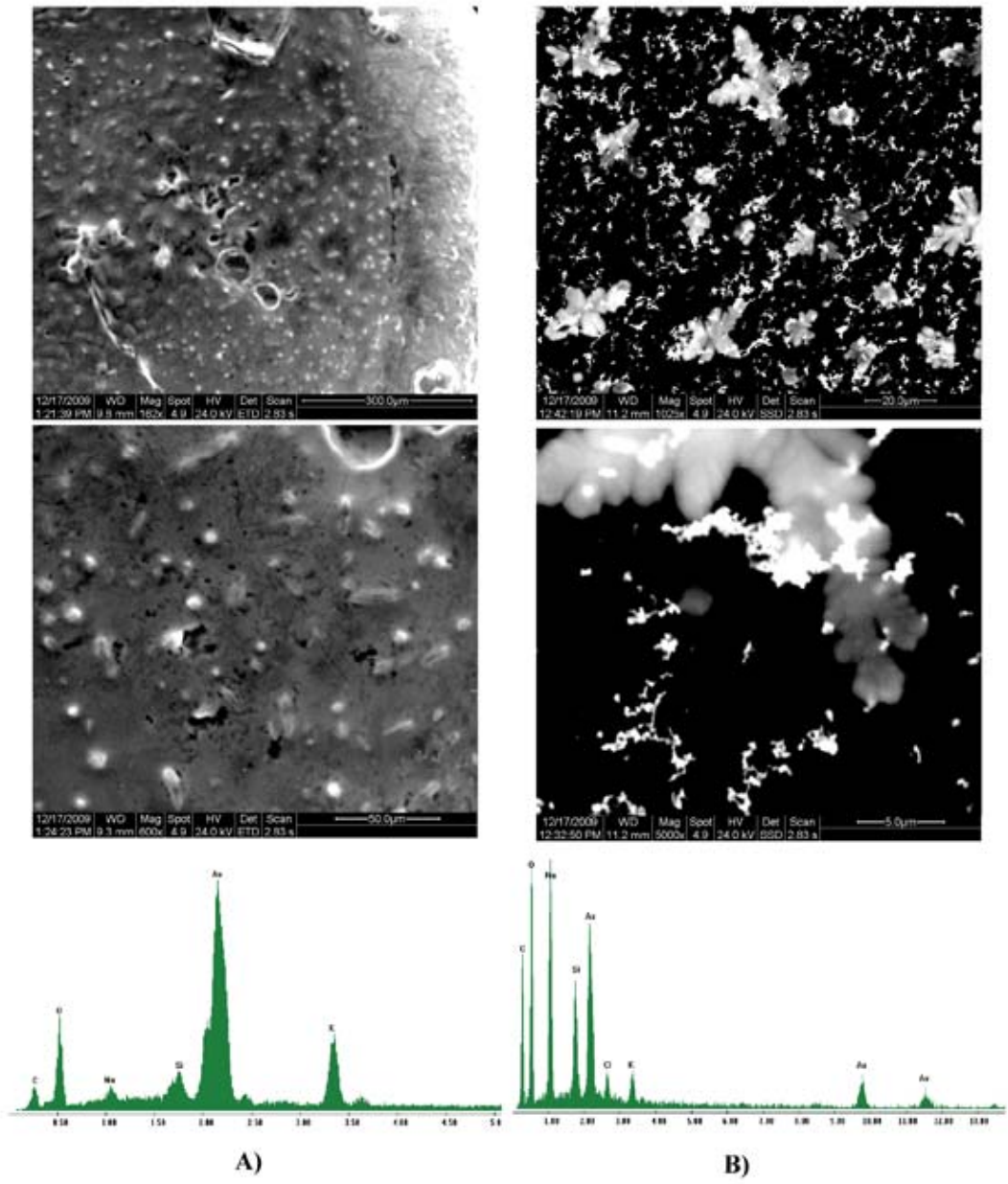

Figure 3.17: SEM micrographs and the EDS spectra corresponding to the AuNPs(SN2-5 µL)-modified SNGC electrode: A) used and B) not used.

As general conclusions, some aspects should be remarked:

1. The use of the amperometric device, either modified or unmodified, causes erosion of the electrode surface in the form of holes and fissures. When the electrode has not been used, the erosion decreases. Morevoer, there is no significant volume contraction during the gelification step, what is very important for the mechanical stability of the electrode.

2. When using one of the AuNPs-modified electrochemical sensors developed throughout this research work, the gold nanoparticles remain attached to the electrode surface even after many measurements and without the presence of some protective agent or membrane.

3. Finally, the backscattered detector is a very powerful tool to help us to identify different phases according to the qualitative chemical composition of the electrode surface.

Finally and to finish with the SEM and EDS studies, a structural characterization was carried out taking into account the changes suffered by the electrode surface after applying a sequence of the different procedures to which each electrodes is subjected. The normal sequence would be: i) polishing; ii) polarization in H_2SO_4 0.05 M (5 cycles); iii) deposition of the required volume of the Au colloidal solution (3 or 5 µL); iv) employment of the electrode to obtain a calibration curve (at least 54 measurements).

Thus, the samples investigated were distributed as follows:

1. Bare Sonogel-Carbon electrode polished and polarised.

2. Bare Sonogel-Carbon electrode polished and not polarised.

3. Bare Sonogel-Carbon electrode polished, polarised, coated with 5 µL of AuNPs from synthesis 1, and used.

4. Bare Sonogel-Carbon electrode polished, polarised, coated with 5 µL of AuNPs from synthesis 1, and not used.

5. Bare Sonogel-Carbon electrode polished, polarised, coated with 5 µL of AuNPs from synthesis 2, and used.

6. Bare Sonogel-Carbon electrode polished, polarised, coated with 5 µL of AuNPs from synthesis 2, and not used.

The discussion will be done using these configurations by couples.

- Bare Sonogel-Carbon electrode polished (polarised and not polarised).

Figure 3.18 shows the SEM micrographs and the EDS spectra corresponding to these electrodes: one that has been polarised (Figure 3.18 A) and other that has not been polarised (Figure 3.18 B).

In these samples, one of the electrodes has been polarised and the other not. So, here it is intended to establish the effect of the electrochemical polarisation in H_2SO_4 0.05 M on the electrode surface. As it can be extracted from the figures, after polarising the electrode, erosion occurs and holes and fissures appear; hence the active surface of the electrode increases, what justifies the results previously discussed. Moreover, there is also some separation between the material and the capillary tube. When the polarisation is not carried out, the erosion is almost inexistent; the small holes and fissures observed correspond to the polishing step. The EDS spectrum is normal in both cases for an unmodified SNGC electrode.

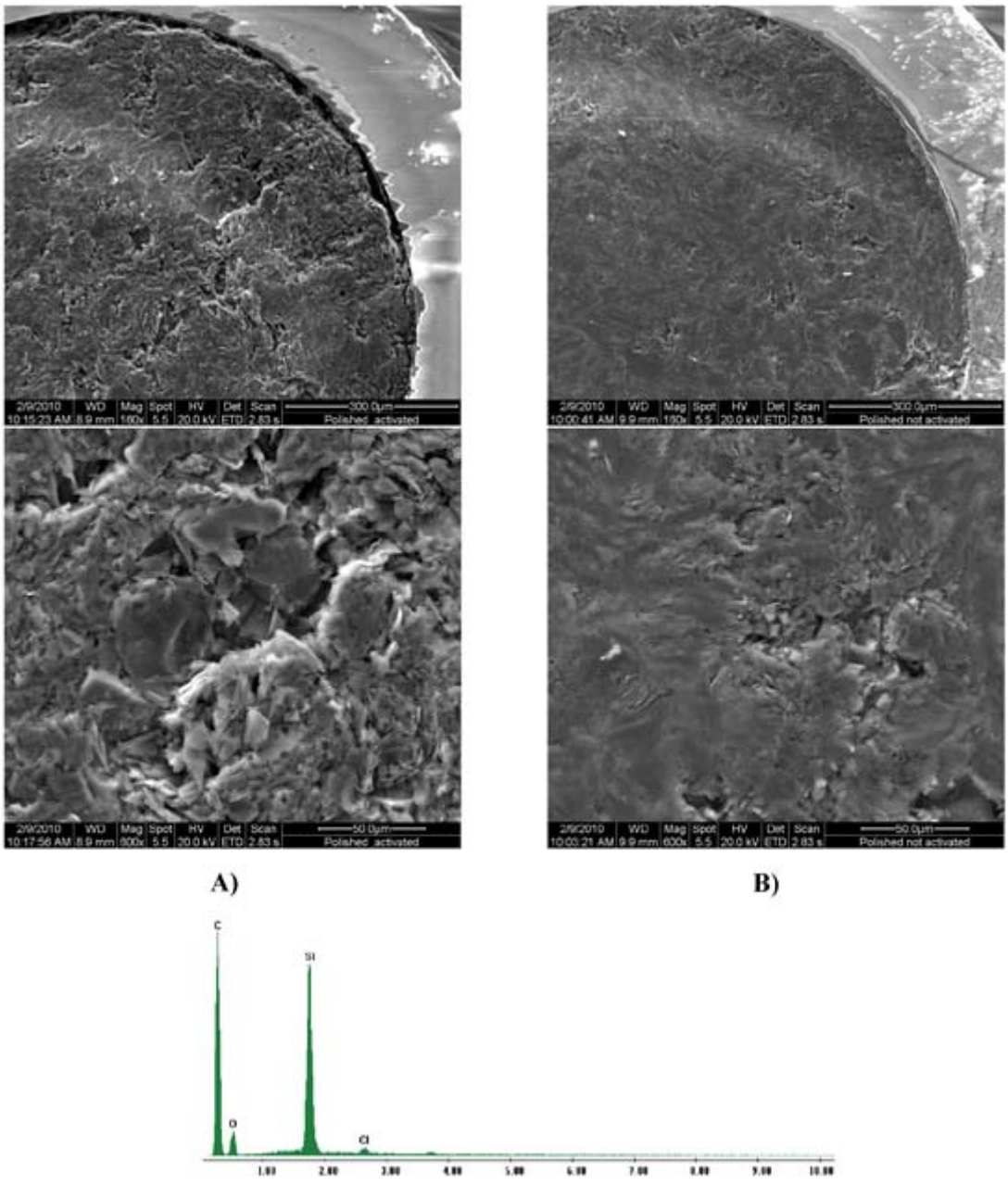

Figure 3.18: SEM micrographs and the EDS spectra corresponding to the bare Sonogel-Carbon electrode polished: polarised A) and not polarised B).

- Bare Sonogel-Carbon electrode polished, polarised, and coated with 5 µL of AuNPs from synthesis 1 (used and not used).

Figure 3.19 shows the SEM micrographs and the EDS spectra corresponding to these electrodes: one used (Figure 3.19 A) and other not used (Figure 3.19 B). In this case,

the backscattered detector has been employed (second images); that is why the presence of gold nanoparticles on the electrode surface is easily evidenced (white brilliant aggregates). EDS spectra corroborates the presence of Au in both cases, as well as some impurities of Na and Cl in the form of crystals, that have the same origin as discussed previously and that appear fundamentally on the surface of the electrode not used. Furthermore, this electrode seems to show more gold nanoparticles on its surface, what indicates that after the use, some gold nanoparticles are desorbed. When looking at the micrographs for the electrode used, holes and fissures due to its utilization can be noticed.

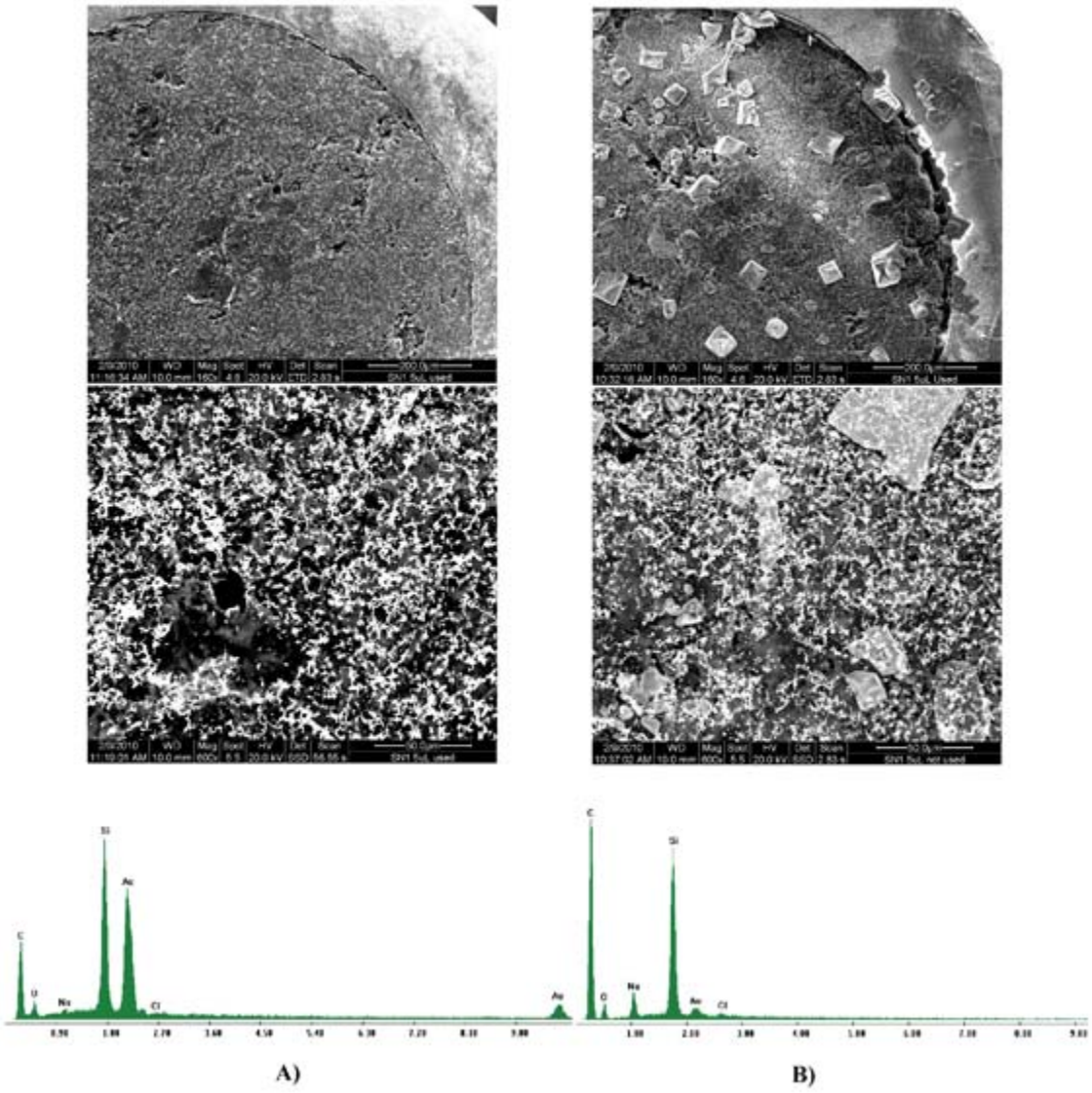

Figure 3.19: SEM micrographs and the EDS spectra corresponding to the bare Sonogel-Carbon electrode polished, polarised, and coated with 5 µL of AuNPs from synthesis 1: used A) and not used B).

- Bare Sonogel-Carbon electrode polished, polarised, and coated with 5 µL of AuNPs from synthesis 2 (used and not used).

Figure 3.20 shows the SEM micrographs and the EDS spectra corresponding to these electrodes: one used (Figure 3.20 A) and other not used (Figure 3.20 B).

Similar considerations to the previous samples can be made here: the presence of crystals from the buffer in the electrode not used; and the existence of a great amount of nanoparticles on the surface, much higher when the electrode is not used and evidenced thanks to the use of the SEM in the backscattered mode. For the electrode used, the typical holes and fissures due to its utilization can be clearly observed. EDS spectra tell us that the electrode not used shows more impurities on its surface than the electrode used, which present the typical composition of a SNGC material modified with gold nanoparticles.

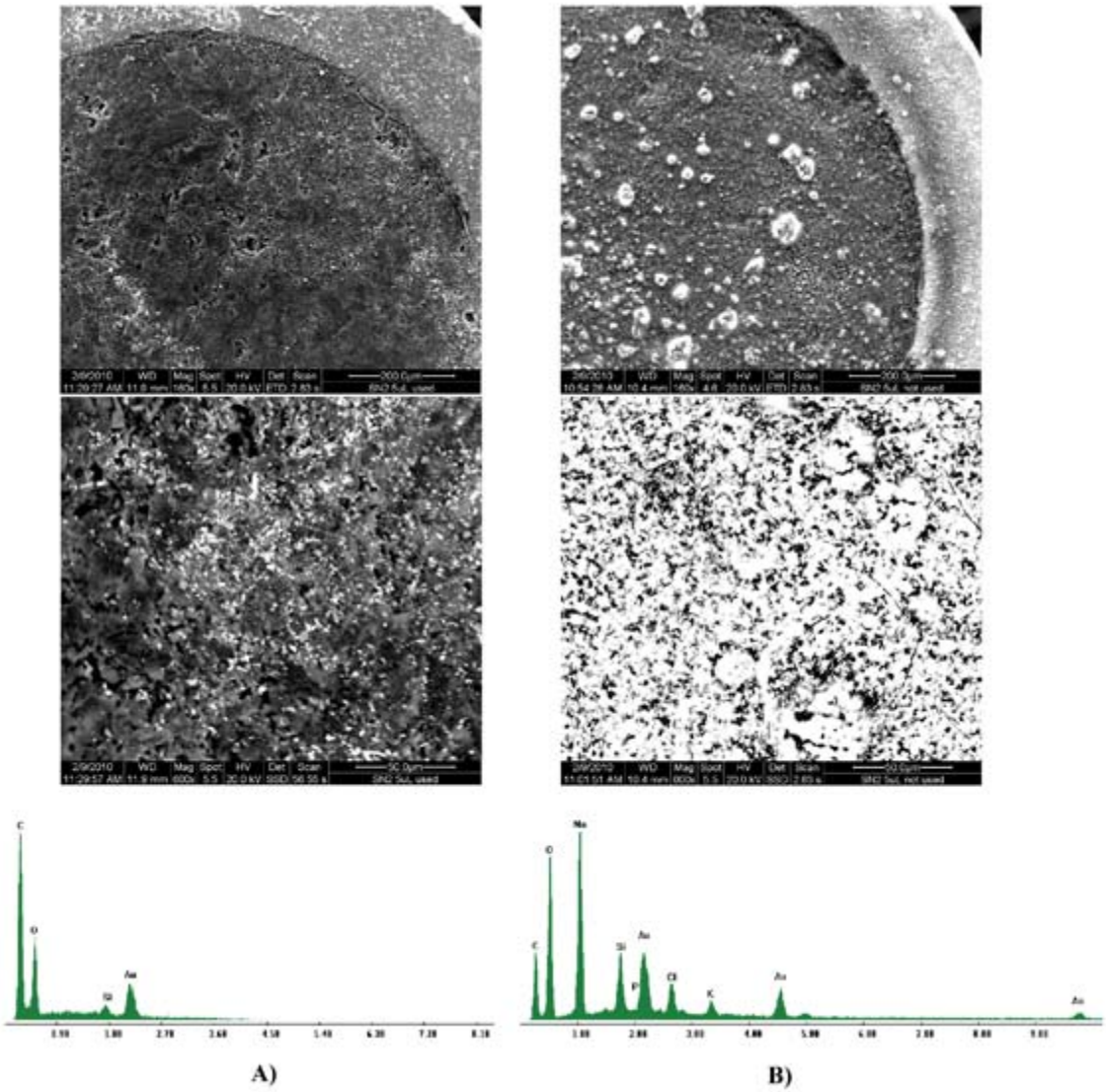

1Figure 3.20: SEM micrographs and the EDS spectra corresponding to the bare Sonogel-Carbon electrode polished, polarised, and coated with 5 µL of AuNPs from synthesis 2: used A) and not used B).

The general conclusions outlined previously are also valid here.

3.3.3. Transmission electron microscopy (TEM).

The morphology, shape and size distribution of gold nanoparticles from the two synthetic routes: thermal (SN1) and ultrasonic (SN2) were studied by transmission electron microscopy (TEM).Christine *et al.* [90] gives us information about the gold nanoparticles synthesized by the thermal method (SN1). Au nanoparticles prepared according to this protocol were nearly spherical, with average diameters of 12–13 nm (standard deviations about ± 1.5 nm).

With respect to the gold nanoparticles synthesized by the ultrasonic method (SN2), they show a spherical shape as seen in Figure 3.21. Moreover, the size is very homogeneous, with a size distribution between 5 and 17 nm (Figure 3.22). More than 90% of the AuNPs shows a diameter ranking from 7 to 13 nm. The average size is 11 ± 1 nm.

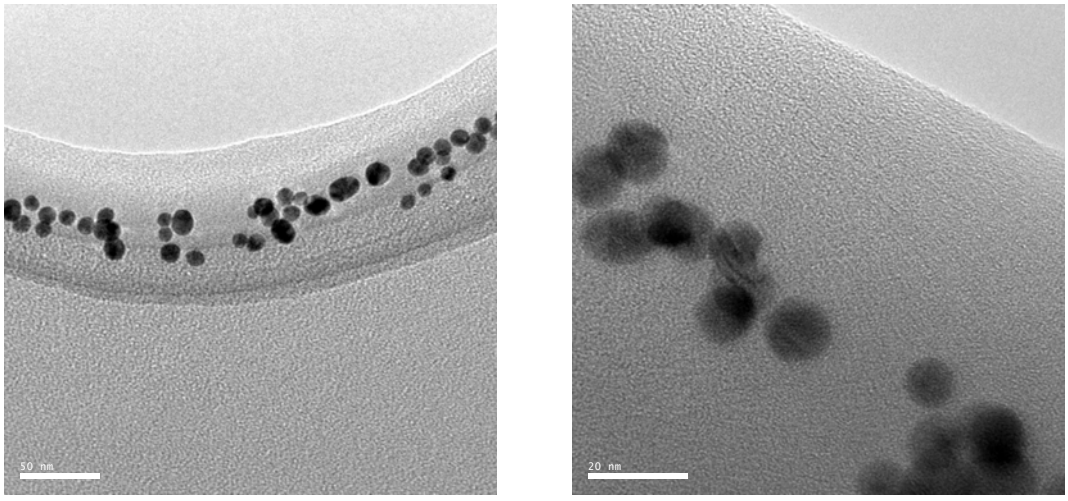

Figure 3.21: TEM micrographs corresponding to the gold nanoparticles synthesized by the ultrasonic method (SN2).

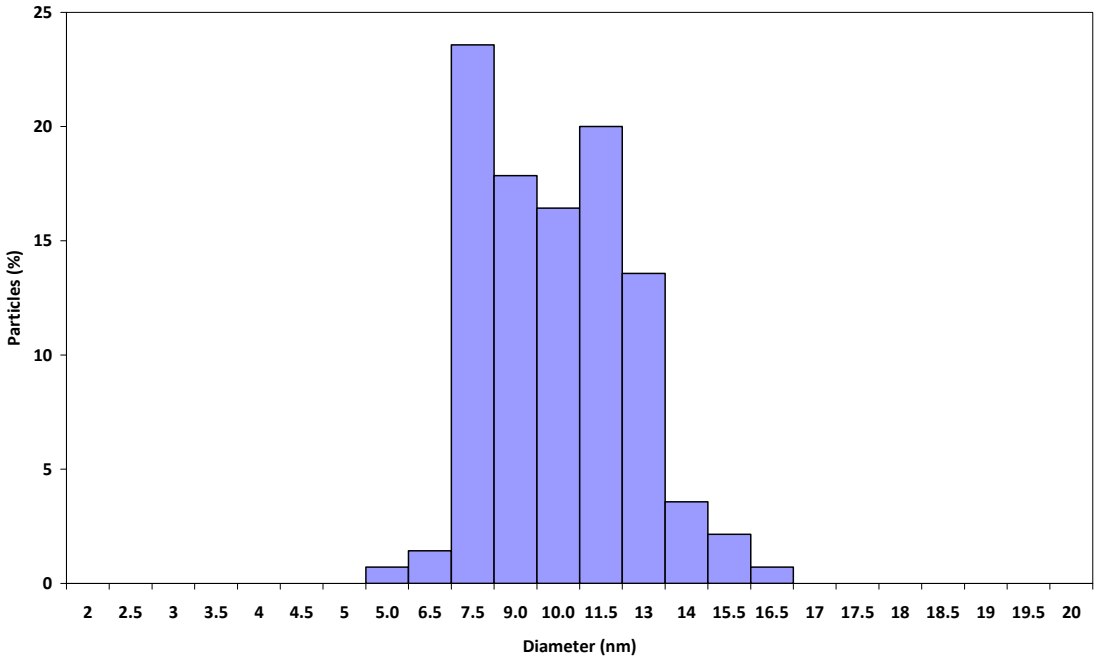

Figure 3.22: Size distribution of the gold nanoparticles synthesized by the ultrasonic method (SN2).

3.4. Real Sample analysis

The research study also includes the first attempts for the application of the amperometric sensors developed throughout this research work to real samples. Some tests have been done to determine ascorbic acid (vitamin C) in apple juices for babies.

12.5 mL of phosphate buffer solution (0.2 M, pH=6.90) with 12.5 mL of the apple juice from local source (labelled concentration = 100 ppm) were transferred into an electrochemical cell, and then the electrode system was immersed into the solution. The experiment was carried out at optimized DPV conditions (see section 3.2.2).

The determination of AA in the sample was carried out by following two different strategies: i) calibration curve and ii) the standard addition method in order to prevent any matrix effect.

With respect to the first strategy, the results were not good. The best recovery percentages were obtained for AuNPs(SN2)-modified Sonogel-Carbon electrodes: from 75 to 78 %. The main reasons for that can be given as follows:

- Excessive use of the electrodes.
- Passivation of the electrode surface due to other chemical species in the apple juice matrix.
- The calibration curve used was not performed taking into account the matrix effect.

Regarding the standard addition method, more appropriate for measuring real samples, since it takes into account the matrix effect, gives slightly better recovery percentages. Table 3.9 shows the experimental results obtained for the real sample measurements using this strategy.

Table 3.9: Experimental results for the determination of AA in apple juice for babies by using the standard addition method.

Electrode	Real sample (ppm)	Measured (ppm)	Recovery (%)
AuNPs(SN1-3 µL)-modified SNGC electrode	100	129	129
AuNPs(SN2-5 µL)-modified SNGC electrode	100	117	117
AuNPs(SN2-3 µL)-modified SNGC electrode	66	47	71

The best recovery percentage values are shown in the table, as well as the configuration of the electrodes used for the measurements. The AuNPs(SN2-5 µL)-modified SNGC electrode offers the best results for the real sample.

Perhaps, in this case, as we have employed electrodes that have been used many times, the results are not the expected ones. That stress may have lead to loss in sensitivity.

Nevertheless, this is a first attempt to try these amperometric devices in real samples. Further studies need to be done in future work.

4. Conclusions.

In this research work, new amperometric sensors were developed. These devices were modified with the incorporation of gold nanoparticles produced directly by simple reduction of Au(lll) with sodium citrate, which controlled the particle size. UV-Visible spectroscopy was used to study the time stability of these gold nanoparticles. The reduction of Au^{3+} to Au^{0} showed strong absorption peaks that remained near to 525 nm after 30 days for the two syntheses employed (thermal: SN1, and ultrasonic: SN2), indicating the formation of gold nanoparticles.

The electrochemical behaviour of the sensors was investigated by employing Cyclic Voltammetry (CV) and Differential Pulse Voltammetry (DPV). Cyclic voltammetric results shows that the redox peak currents of all Sonogel-Carbon electrodes studied, increased linearly with the square root of scan rate indicating that electrochemical reactions are controlled by diffusion process. The reversible nature of the process was evident from the analysis of CV data of all the Sonogel-Carbon electrodes. The C_{obs} value for the unmodified electrode shows perfect correspondence with previously published results. The presence of gold nanoparticles in the electrode surface increases the capacity values, as expected; the higher the amount of AuNPs on the electrode surface, the higher the capacity values as well. Moreover, the modification of the electrode surface with gold nanoparticles increases the number of electroactive sites, and hence, the current peak of the analytes measured.

Differential Pulse Voltammetry (DPV) was used to evaluate and demonstrate the good electrochemical performance of our devices when determining ascorbic acid; the effects of the DPV parameters on the response of the electrodes was studied by means of three factors and three level Box-Behnken experimental design. The optimization of DPV parameters required for maximizing the sensitivity of the devices was presented. Furthermore, the modified Sonogel-Carbon electrodes developed showed good reproducibility and repeatability; these parameters also

increased with the amount of AuNPs on the electrode surface. The detection and quantification limits were also calculated.

Finally, regarding the structural characterization, the morphology of the AuNPs-modified Sonogel-Carbon electrodes was studied with Optical Microscopy (OM), Transmission Electron Microscopy (TEM), Scanning Electron Microscopy (SEM) and X-ray Energy Dispersive Spectroscopy (EDS). The structural characterization was also carried out taking into account the changes suffered by the electrode surface after applying a sequence of the different procedures to which each electrodes is subjected.

After applying these techniques and on one hand, it can be concluded that the use of the electrode causes certain erosion of the electrode surface, in the form of holes and fissures, so that the lower the erosion, the better the mechanical stability of the amperometric devices. On the other hand, characterization techniques gave us information about the link of the gold nanoparticles on the electrode surface: this link seems to be strong enough to maintain them attached to the electrode surface even after many measurements and without the presence of some protective agent or membrane.

The amperometric sensors employed here were also applied to determine ascorbic acid in apple juice for babies, giving regular results, mainly due to the stress suffered by the electrodes since they had been used many times.

As a final and general conclusion, it can be said that thanks to the electrochemical and structural characterizations, it has been demonstrated that the AuNPs-modified Sonogel-Carbon electrodes can be applied successfully as amperometric sensor devices. They show good electrochemical properties concerning sensitivity, capacity, reproducibility, repeatability and detection and quantification limits versus a benchmark analyte: ascorbic acid.

5. Future work.

In future work many investigations should be accomplished closely related to the present research work:

1. To improve the modification of the amperometric devices by coating the electrode surface with some polymeric materials such as polyethyleneglycol and Nafion® after the deposition of gold nanoparticles. These substances can act as protective membranes to avoid leakage of the nanoparticles from the electrode surfaces.

2. To use a third synthetic route of gold nanoparticles to compare with those employed in this work in order to test the performance of the electrochemical device.

3. To test the performance of Sonogel-Carbon electrodes modified during their synthesis with gold nanoparticles, *i.e.*, to insert the AuNPs into the Sonogel matrix instead of depositing them on its surface.

4. To enhance the electrochemical characterisation by studying the mechanisms corresponding to other analytes (AA and Hexamine trichlororuthenium(lll)) in cyclic voltammetry.

5. To use these devices to determine other kinds of analytes such as environmental pollutants (Chlorophenols) or Polyphenols, among others.

6. To improve the structural characterisation by using other techniques such as Atomic Force Microscopy (AFM), Scanning Electrochemical Microscopy (SECM), among others.

7. To deepen the real sample studies in order to obtain good amperometric devices useful for quality control of foods and environmental samples.

6. References

1. Nanoparticles. From theory to application, (Günter Schmid Ed.), Wiley-VCH Verlag GMBH & Co. KgaA: Weinheim, Germany, **2006**.
2. Nanostructured materials and nanotechnology, Concise ed., (Hari Singh Nalwa.Ed.), Academic Press: California, USA, **2002**.
3. M. M. Cordero-Rando, Ignacio Naranjo-Rodriguez, J. M Palacios-Santander, L. M Cubillana-Aguilera and J.L.Hidalgo-Hidalgo-de-Cisneros. *Electroanalysis* **2005**, *17(9)* 806-813.
4. M. A. Kim, W. Y. Lee. *Anal. Chim. Acta* **2003**, *479*, 143.
5. P. C. Chiang, W. T. Whang. *Polymer* **2003**, 44, 2249.
6. X. Yang, L. Hua, H. Gong, S. N. Tan. *Anal. Chim. Acta* **2003**,478, 67.
7. S. S. Rosatto, P. T. Sotomayor, L. T. Kubota, Y. Gushikem. *Electrochim. Acta* **2002**, 47;4451.
8. G.Gun, M. Tsionsky and O.Lev. *Anal. Chim. Acta* **1994**, *294*, 261-270.
9. P. V. A.Pamidi; C.; S. A. ParradoKane; J.Wang; M.R.Smith; J.M.Pingarrón. *Talanta* **1997**, 44, 1929-1934.
10. B.Dunn,G.C. Farrington, B. Katz. *Solid State Ionics* **1994**, *70/71*, 3-10.
11. J. L. Hidalgo-Hidalgo-de-Cisneros, M. M. Cordero-Rando, I. Naranjo-Rodríguez, E. Blanco-Ollero, L. Esquivias-Fedriani, *Patente P200100556*, España (**2001**).
12. M. M. Cordero-Rando, J. L. Hidalgo-Hidalgo-de-Cisneros, E. Blanco, I. Naranjo-Rodríguez. *Anal. Chem*., **2002** 74, 2423.

13. B. Ballarin, C. Zanardi, L. Schenetti, R. Seeber, J. L. Hidalgo-Hidalgo-de-Cisneros, *Synth. Met.*, **2003**,139(1);29.

14. B. Ballarin, M. Gazzano, J. L. Hidalgo-Hidalgo-de-Cisneros, D. Tonelli, R. Seeber, *Anal. Bioanal. Chem.*, **2002**, 374, 891.

15. B. Ballarin, M. M. Cordero-Rando, E. Blanco, J. L. Hidalgo-Hidalgo-de-Cisneros, R. Seeber, D. Tonelli. *Collect. Czech. Chem. Commun.*, **2003**, 68,1420.

16. M. El Kaoutit, L. M. Cubillana-Aguilera, I. Naranjo-Rodríguez, J. M. Palacios-Santander, K Tensamani, J. L. Hidalgo-Hidalgo-de-Cisneros. *Biosensors and Bioelectronic*, **2007**,22,2958-2966.

17. J. M. Palacios-Santander, M. Cocchi, A. Ulrici, I. Naranjo-Rodríguez, R. Seeber, J. L. Hidalgo-Hidalgo-de-Cisneros. Chemometrics and Intelligent Laboratory Systems, **2008**,91, 110–120.

18. J. M. Palacios-Santander, A. Jiménez-Jiménez, I. Naranjo-Rodríguez, L. M. Cubillana-Aguilera, J. L. Hidalgo-Hidalgo-de-Cisneros. *Microchim. Acta*, **2003**,142, 27.

19. A. V. Narasimham. *J. De Physique.* **1979**, 40(11) C8-223.

20. N. V. Malykh, I. A. Ogorodnikov. *J. De Physique, Supl.* ***1979***, 40(11), C8-300.

21. K. S. Suslick. *Pour la science,* **1989**,138,88.

22. S. W. Wong, W. Y. Chon. *AIChE Journal,* ***1969***, 15(2), 281.

23. E. Blanco, L. Esquivias, R. Litrán, M. Piñero, M. Ramírez del Solar, N. De la Rosa Fox. *App. Organometal. Chem.****1999,*** 13(5), 399.

24. Shaojun Guo and Erkang Wang. Review Synthesis and electrochemical applications of gold nanoparticles. *Analytica Chimica Acta.* **2007**, 598, 181–192.

25. L.O. Brown, J.E. Hutchison. *J. Phys. Chem*. **2001**, 105(B), 8911.

26. R. L. Whetten, J. T. Khoury, M. M. Alvarez, S. Murthy, I. Vezmar, Z. L. Wang, P. W. Stephens, C. L. Cleveland, W. D. Luedtke and U. Landman, *Adv. Mater*., **1996**, 8, 428-433.

27. A.Ralph Sperling, Pilar Rivera Gil, Feng Zhang, Marco Zanella and Wolfgang J. Parak. *Chem. Soc. Rev.*, **2008**, 37, 1896–1908.

28. A.Henglein.Sonochemistry; Historical developments and modern aspects.Ultrasonics,**1985**,25,6-16.

29. K.S.Suslick,In Ultrasound,Its Chemical,Physical and Biological Effects(K.S.Suslick,Ed.);VCH publishing: Weinheim,1988; pp 138-146.

30. D.Bremner,Historical introduction to sonochemistry,In Advances in sonochemistry Vol.1; (T.J.Mason,Ed); JAI press: London,1990; pp.9-20.

31. P. Riesz,Frec radical generation by ultrasound in aqueous solution of volatile and non-volatile solutes ln Advances in sonochemistry Vol.2;(T. .J Mason,Ed.); JAI Press: London,**1991**; pp 24-64.

32. P .Riesz and T. Kondo. *Free radical Biol.Med*. **1992**,13,247-270.

33. Juncheng Liu,Gaowu Qin, Poovathinthodiyil Raveendran and Yukata Ikushima. *Chem. Eur. J.* **2006**, 12, 2131 – 2138.

34. Wen Yang, Ying Ma, Jiang Tang, Xiurong Yang. *Physicochem. Eng. Aspects* **2007**,302, 628–633.

35. O. Siiman, A. Burshteyn, *US Patent* .**1993**,5(240),640.

36. H. Huang, X. Yang. *Carbohydrate Res.* **2004**, 339,2627.

37. H. Huang, X. Yang. Biomacromolecules. **2005**, 5,2340.

38. Y. Ma, N. Li, C. Yang, X. Yang. *Anal. Bioanal. Chem.* **2005**,382, 1044.

39. P. Raveendran, J. Fu, S.L. Wallen. *Green. Chem.* **2007**,8, 34.

40. Yong Jin, Pingjun Wang, Donghong Yin, Jianfu Liu, Liangsheng Qin,Ningya Yu, Guoyong Xie and Biaomo Li.*Colloids and Surfaces A: Physicochem. Eng. Aspects*, **2007**, 302, 366–370.

41. P. Cintas, J.-L. Luche. *Green Chem*., **1999**, 115–125.

42. Y.G. Adewuyi. *Ind. Eng. Chem. Res.***2001**, 40, 4681–4715.

43. Kenneth S. Suslick and Gareth J. Price. Annu. *Rev. Mater. Sci*., **1999**,29:295–326.

44. Van der Hoff BME, Glynn PAR. *J.Macromol. Sci. Macromol.* Chem.*,***1974**. A8:429.

45. K. S. Alber, J. A. Cox. *Microchim. Acta,* **1997**, 127,131.

46. C. Malins, H. G. Glever, T. E. Keyes, J. G. Vos, W. J. Dressick, B. D. MacCraith, *Sens. Actuators B*, **2000**), 67,89.

47. M. A. Macêdo, M. A. Aegerter. *J. Sol-Gel Sci. Technol.,***1994**, 2, 667.

48. A. E. Aliev, H. W. Shin. *Solid State Ion*., **2002**,425,154-155.

49. A. Walkarius. *Electroanalysis,* **1998**,10(18), 1217.

50. P. Ganesan, H. Colon, B. Haran, B. N. Popov. *J. Power Sources*, **2003**,115,12.

51. J. Seneviratne, J. A. Cox. *Talanta,* **2000**,52, 801.

52. S. V. M. de Moraes, J. B. Passos, P. Schossler, E. B. Caramão, C. C. Moro, T. M. H. Costa, E. V. Benvenutti. *Talanta*, **2003**,59(5), 1039.

53. C. A. Lundgren, R. W. Murray, *J. Electroanal. Chem.,***1987**, 227, 287.

54. J. Watson, T. W. Zerda, *Appl. Spectrosc*., **1991**,45,1360.

55. K. Maruszewski, A. Hreniak, J. Czyżewski, W. Stręk. *Opt. Mater*., **2003**,22, 221.

56. M. A. Kim, W. Y. Lee. *Anal. Chim. Acta*, **2003**, 479, 143.

57. C. Hsueh, M.M. Collinson, J. Electroanal. Chem., **1997**, 420, 243.

58. J. Wang, P. Pamidi, V. B. Nascimento, L. Angnes. *Electroanalysis*, **1997**,9, 689.

59. N. de la Rosa-Fox, R. Erce-Montilla, M. Piñero, L. Esquivias. *Opt. Mater*.,**2003**,22,1.

60. W. Que, X. Hu. *Opt. Mater*., **2003**, 22,31.

61. Y. Guo, A. R. Guadalupe, *Sens. Actuators B*, **1998**, 46, 213.

62. L. Lvova, S. S. Kim, A. Legin, I. Vlasov, J. S. Yang, G. S. Cha, H. Nam. *Anal. Chim. Acta*, **2002**,468,303.

63. M. Badea, A. Amine, G. Palleschi, D. Moscone, G. Volpe, A. Curulli. *J. Electroanal. Chem.*, **2001**, 509, 66.

64. L. Esquivias, N. de la Rosa-Fox, M. Bejarano, M. J. Mosquera, *Langmuir*, **2004**, 20, 3416.

65. D. R. Vollet, D. A. Donatti, A. Ibáñez Ruiz, H. Maceti. *J. Non-Cryst. Solids*, **2003**,324, 201.

66. C. Vix-Guterl, I. Alix, P. Gibot, P. Ehrburger. *Appl. Surf. Science*, **2003**, 210, 329.

67. R. Janes, L. J. Knightley, C. J. Harding. *Dyes & Pigments*, **2004**, 62,199.

68. P.T.Kissinger, *Laboratory Techniques in Electroanalytical Chemistry,* W.R.Heineman (Ed); *Marcel Dekker: New York*, **1984**.

69. D. Schuetzle, R. Hammerle.*Fundamentals and Applications of Chemical Sensors, ACS Symposium Series 309, American Chemical Society*, Washington DC **1986**.

70. G. Gun, M. Tsionsky, O. Lev, *Anal. Chim. Acta*, **1994**, 294, 261.

71. A. W. Robards, A. J. Wilson (Eds.); Procedures in Electron Microscopy, Wiley; EE.UU., **2000**.

72. A. J. Garratt-Reed, D. C. Bell, Energy Dispersive X-ray Analysis in the Electron Microscope, Springer-Verlag Telos, **2002**.

73. John J. Bozzola, Lonnie D. Russell, Electron microscopy. Principles and techniques for Biologists, 2nd ed., Jones and Bartlett Publishers: Massachusetts, USA,**1999**.

74. Joseph Goldstein, Dale Newbury, David Joy, Charles Lyman, Patrick Echlin, Eric Lifshin, Linda Sawyer, and Joseph Michael, Scanning Electron microscopy and X-ray microanalysis, 3rd ed., Springer: New York, USA, **2003**.

75. Laura Cubillana Aguilera, José María Palacios Santander, María Franco Romano, Almoraima Gil Montero, Ignacio Naranjo Rodríguez and José Luis Hidalgo Hidalgo de Cisneros, 'Síntesis verde (ecológica) de sononanopartículas de oro', Patent submitted, Spain, **2010**.

76. L. M. Cubillana-Aguilera, M. Franco-Romano, M. L. A. Gil, I. Naranjo-Rodríguez, J. L. Hidalgo-Hidalgo-de-Cisneros, J. M. Palacios-Santander, 'New procedure for the synthesis of gold nanoparticles based on sonocatalysis', Ultrason. Sonochem., submitted, **2010**.

77. Wong B, Yoda S, Howdle SM. *J Supercrit Fluid*, **2007**, 42, 282.

78. Xie YW, Ye RQ, Liu HL. *Colloids Surf A Physicochem.Eng Asp*, **2006**, 279,175.

79. J.P.Richards,The Chemistry of Gold,Elsevier,Amsterdam,**1978**.

80. Zhu Jian, Wang Yongchang, Plasma Sci. Technol., **2003**, 5(3),1835-1839].

81. Kai Sun,Jingxia Qiu,Jiwei Liu and Yuqing Miao. *J Mater Sci*, **2009**, 44,754–758.

82. A.J.Bard,L.R.Faulkner.Electrochemical methods;wiley Press:New York **1980**; pp.143.

83. M.Wang,X.Xu and j Gao. *J.appl.Electrochem,* **2007**, 37, 705-710.

84. A.Salimi,V.Alizadeh and H.Hadadzadeh.*Electroanalysis, **2004**,* 16, 1984-1991.

85. Mª del Mar Cordero-Rando, José L. Hidalgo-Hidalgo de Cisneros, Eduardo Blanco, and Ignacio Naranjo-Rodríguez, *Anal. Chem.*, **2002**, 74, 2423-2427.

86. B.Ballarin,M.C.Cassani,R.Mazzoni,E.Scavetta and D.Tonelli. *Biosensors and Bioelectronics, **2007**,* 22, 1317-1322.

87. K.Wu,S.Hu,J.Fei and W.Bai. *Anal.Chim.Acta, **2003**,* 489, 215.

88. S. L. C. Ferreira, R. E. Bruns, H. S. Ferreira, G. D. Matos, J. M. David, G. C. Brandao, E. G. P. da Silva, L. A. Portugal, P. S. dos Reis, A. S. Souza, W. N. L. dos Santos, *Analytica Chimica Acta.*, **2007**, 597,179–186.

89. J. C. Miller, J. N. Miller, Estadística para Química Analítica, Addison-Wesley Iberoamericana: Wilmington **1993**, pp. 96 – 98.

90. Christine D. Keating, Michael D. Musick, Melinda H. Keefe, and Michael J. Natan, J. Chem. Educ. **1999**, 76(7), 949-955.